Analysis of Solar, Interplanetary and Ground-based data to study Forbush decreases, Ground Level Enhancements (GLEs) and Geomagnetic storms

Badruddin

Department of Physics
Aligarh Muslim University, Aligarh
India-202 002
✉: badr.physamu@gmail.com

Introduction

- The Sun affects the Earth and its environment in a variety of ways.
- In the Heliosphere, large-scale structure of the solar wind is dominated by two type of disturbance: transient and corotating disturbances.
- Transient disturbances are associated with episodic ejections (Solar Flares/CMEs) of material into interplanetary space from solar regions not previously participating in the solar wind expansion.
- Corotating disturbances (CIRs) are associated with spatial variability in the coronal expansion and solar rotation. CIRs occur in response to the interaction of fast and slow solar winds.

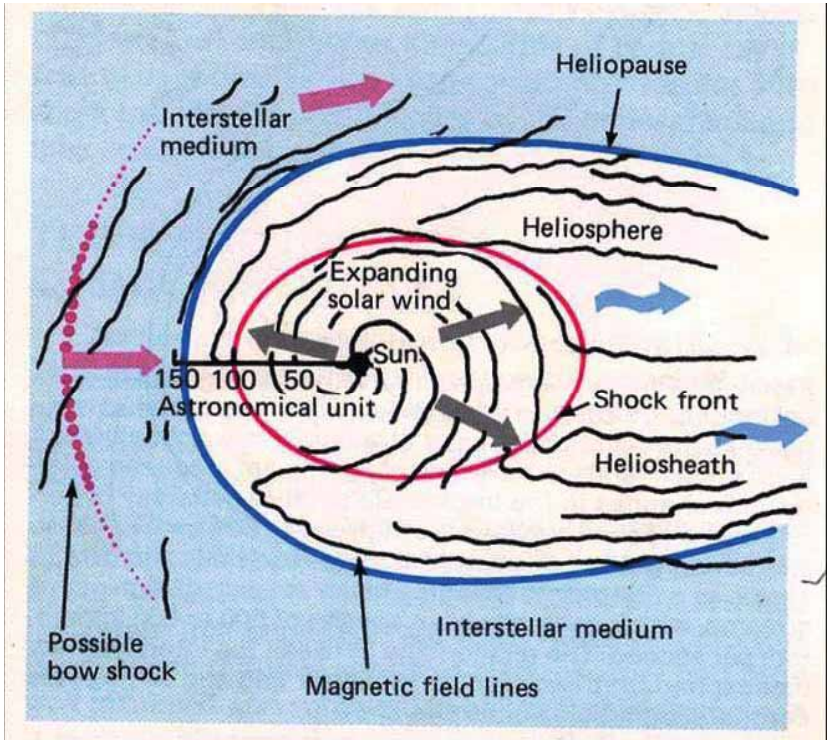

Heliosphere (Venkatesan and Badruddin, 1990)

- ✓ Heliosphere is part of Space that is directly affected by the sun through the solar wind.
- ✓ The region is dominated by the solar magnetic field carried outward by the solar wind plasma

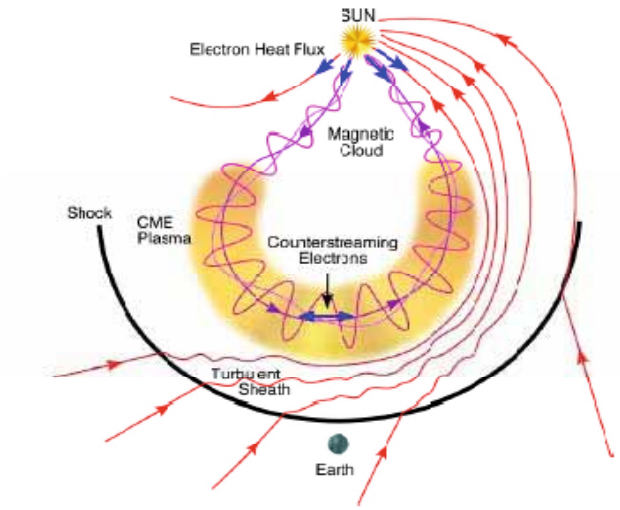

ICME (Richardson and Cane, 2010)

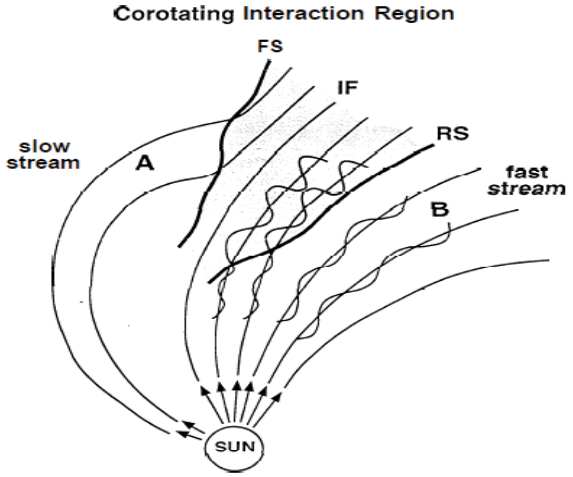

CIR (Gosling, 1990)

➢Flares and CMEs are violent manifestations of solar activity.

➢A Flare is the result of a sudden violent outburst of energy, with energies of up to 10^{25} J being released in the form of charged particles and electromagnetic radiation over a time of some minutes.

➢CMEs are the most spectacular solar eruptions (gigantic magnetic bubbles) expanding outward from the sun, rip out billions of tens of material from the corona hurling it into interplanetary space in expanding magnetic bubbles.

These solar/interplanetary disturbances generate;

- Geomagnetic Storms (GS) in Earth's magnetic environment
- Forbush decreases (FDs) in GCR intensity in the Heliosphere and on the Earth.
- Solar Energetic Particles (SEPs) in the Heliosphere and ground level enhancements (GLEs) on the Earth.

➢There is striking similarity between the time profile (shape) of large Forbush decreases and major geomagnetic storms - although one-to-one correspondence is not so obvious - probably due to different mechanism.

➢ Precursor anisotropies before the arrival of an interplanetary shock and subsequent FD have been detected in ground based GCR intensity measurements by neutron monitors and muon detectors- providing advance impact of shocks/CMEs at the Earth's magnetosphere (GS).

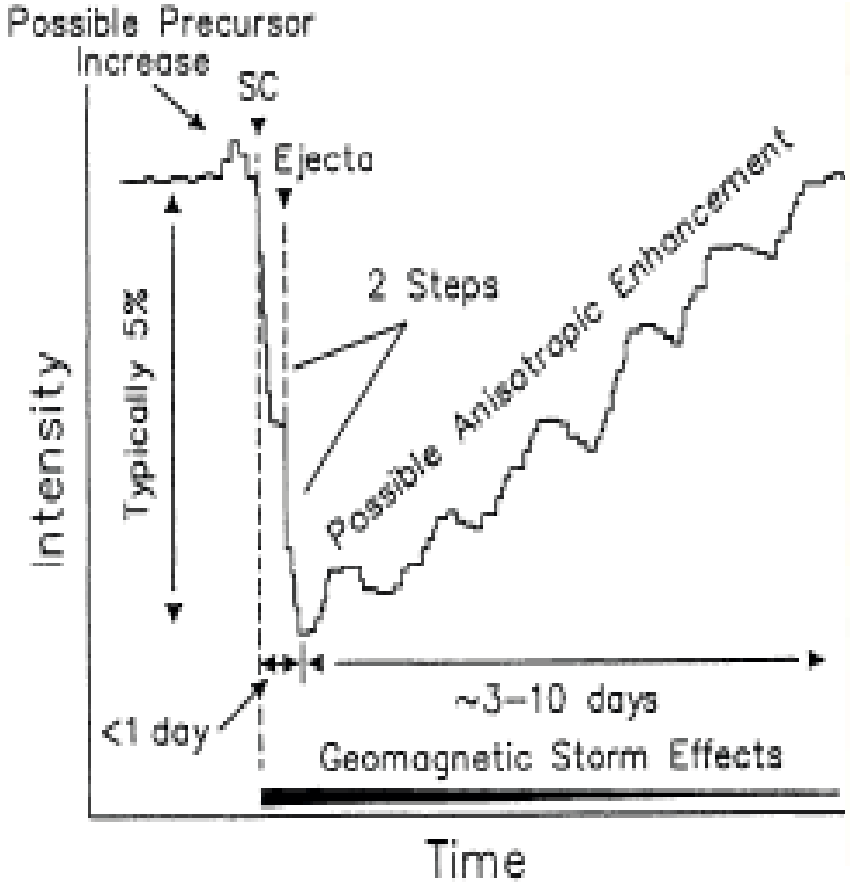

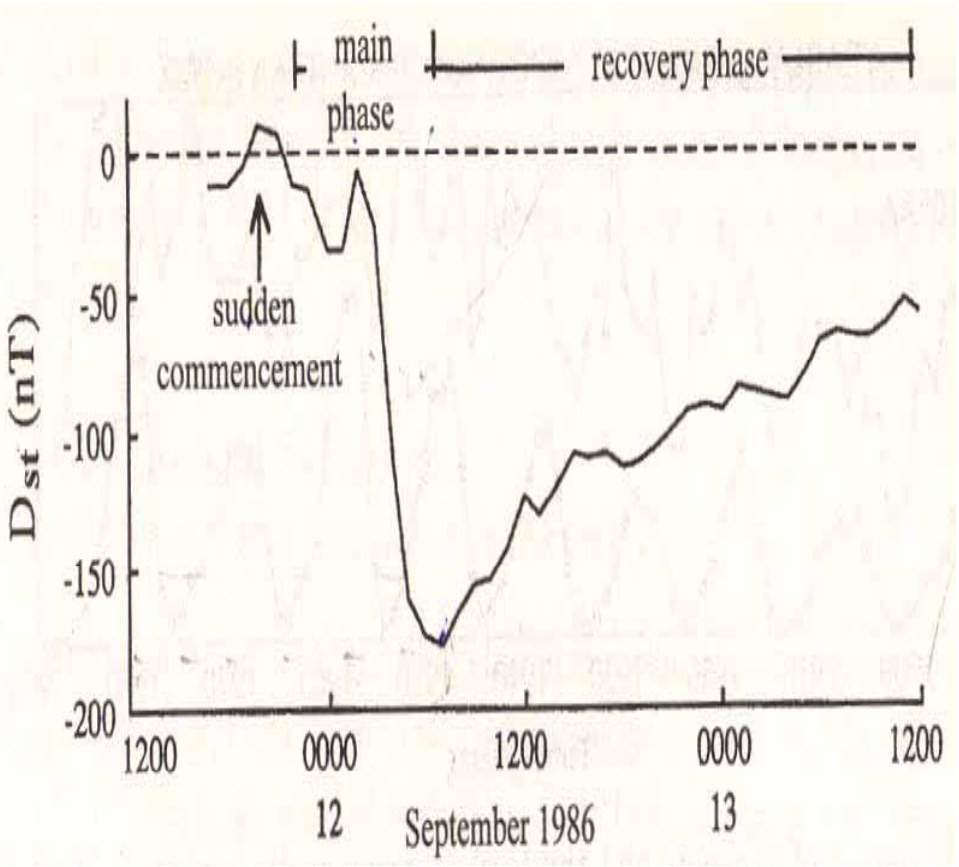

Schematic representation of Forbush decrease/GS showing the main features

SPACE WEATHER PERSPECTIVE

- Space weather originates from the Sun
- Space weather effects arise from the dynamic conditions in the Earth's space environment driven by processes on the sun.
- Understanding of the processes involved near the sun, the interplanetary space and in the near- Earth environment can be enhanced with the targeted study of the combination of spacecrafts observations of Sun, interplanetary space and ground-based observations of near-earth phenomena.
- It is important to enhance the physical understanding to solar process, so that predictions can be made using solar observations to gain more lead time.
- Identifying the plasma/field conditions in solar active regions, evolution and propagation of solar eruptions and ultimately their effectiveness as regards their space weather consequences is important.
- Research directed towards physical understanding of solar, interplanetary and magnetospheric processes and phenomena will ultimately lead to our capability of space weather forecast both in terms of accuracy and lead time.

Geomagnetic Storms

- Perturbation of the Earth's magnetic field.
- Result as a final element of a chain of processes that starts on the Sun, affects the solar wind and the interplanetary medium, and end on the earth.
- Key question in the scientific community is the ability to predict the occurrence of GS on the basis of solar and interplanetary observations.
- GS owes its origin to physical processes in which energy transferred from the solar wind to the earth's magnetosphere is redistributed in the magnetosphere-ionosphere coupled system in the form of electric currents.
- CMEs are the main sources of geomagnetic storms.

All the ICMES are not geoeffective; the important questions are:

- How to distinguish those events that are geoeffective from those that are not?
- How can we forecast the arrival of geoeffective ICMEs?

- A major aim of space weather research is to identify the interplanetary drivers (e.g. Shock/Sheath/ICMEs/MCs/CIRs/SIRs) of major geomagnetic storms, and their solar counter parts (e.g. CMEs, High Speed Streams from Coronal Holes etc) and their specific features as regards their geoeffectiveness.
- The underlying mechanism that is responsible for generating these storms due to different sources has to be identified unambiguously.
- Major Geomagnetic storms are among the most important space weather phenomena.
- The interaction of the solar wind disturbances with the Earth's magnetosphere can produce disturbances, and at times complete disruptions, of technological systems, on the earth and in the Space around the Earth.
- Loss cone precursor anisotropy - CR deficit-when detector is magnetically connected to CR-depletion region down streams of IP shock. CR anisotropy enhancements provide continuous real time monitoring of the variation of CR-density and anisotropy in the interplanetary space which is important for eventual alerts of geomagnetic disturbances

Different Events Analyzed

- December 2006 → GS-3, FDs-2, GLE-1
- January 2005 → GS-5, FDs-3, GLE-1
- April 2001 → GS-7, FDs-4, GLE-1
- July 2000 → GS-4, FDs-4, GLE-1

Time variation (hourly data) of Dst (nT), V(km/s), B (nT), its north-south component (B_z) and the product B_zV^2 during December 2006.

GS1: Dst: -55 nT
Structure: Two step storm
Solar Source: HSS from CH
Interplanetary structure: CIR
Plasma/field parameter:
B_Z: - 8.9 nT, E_y: 4.10 mV/m

GS2: Dst: -55 nT
Structure : Two step storm
Solar Source: ?
Interplanetary structure: ?
Plasma/ field parameter:
B_Z: - 5.1 nT, E_y: 3.74 mV/m

GS3: Dst: -162nT
Structure : Two step storm
Solar Source: CME
Interplanetary structure: Sheath, MC
Plasma/field parameter: B_Z: -15.7 nT, E_y: 13.56 mV/m

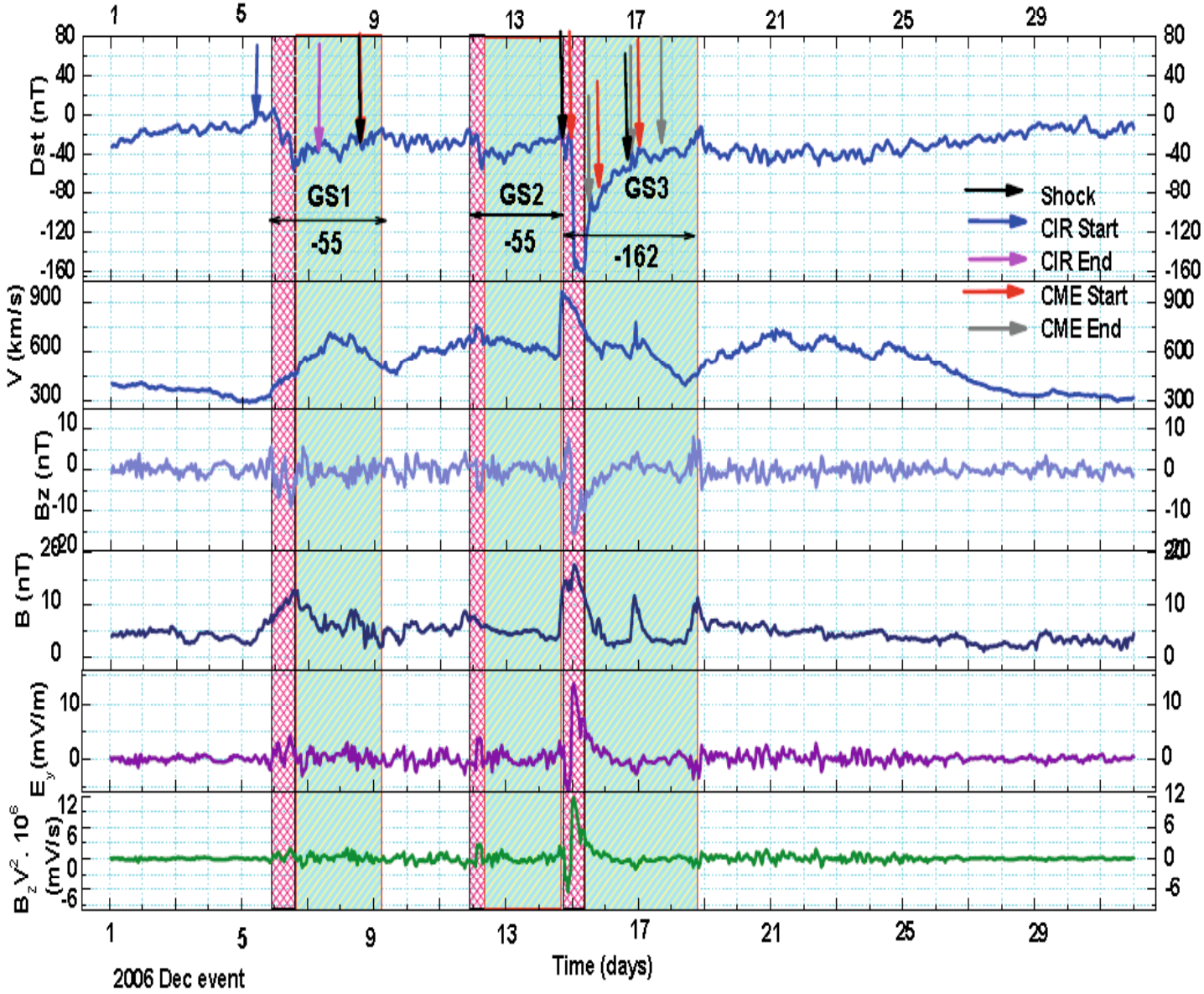

Time variation (hourly data) of Dst (nT), V(km/s), B (nT), its north-south component (B_z) and the product B_zV^2 during January 2005.

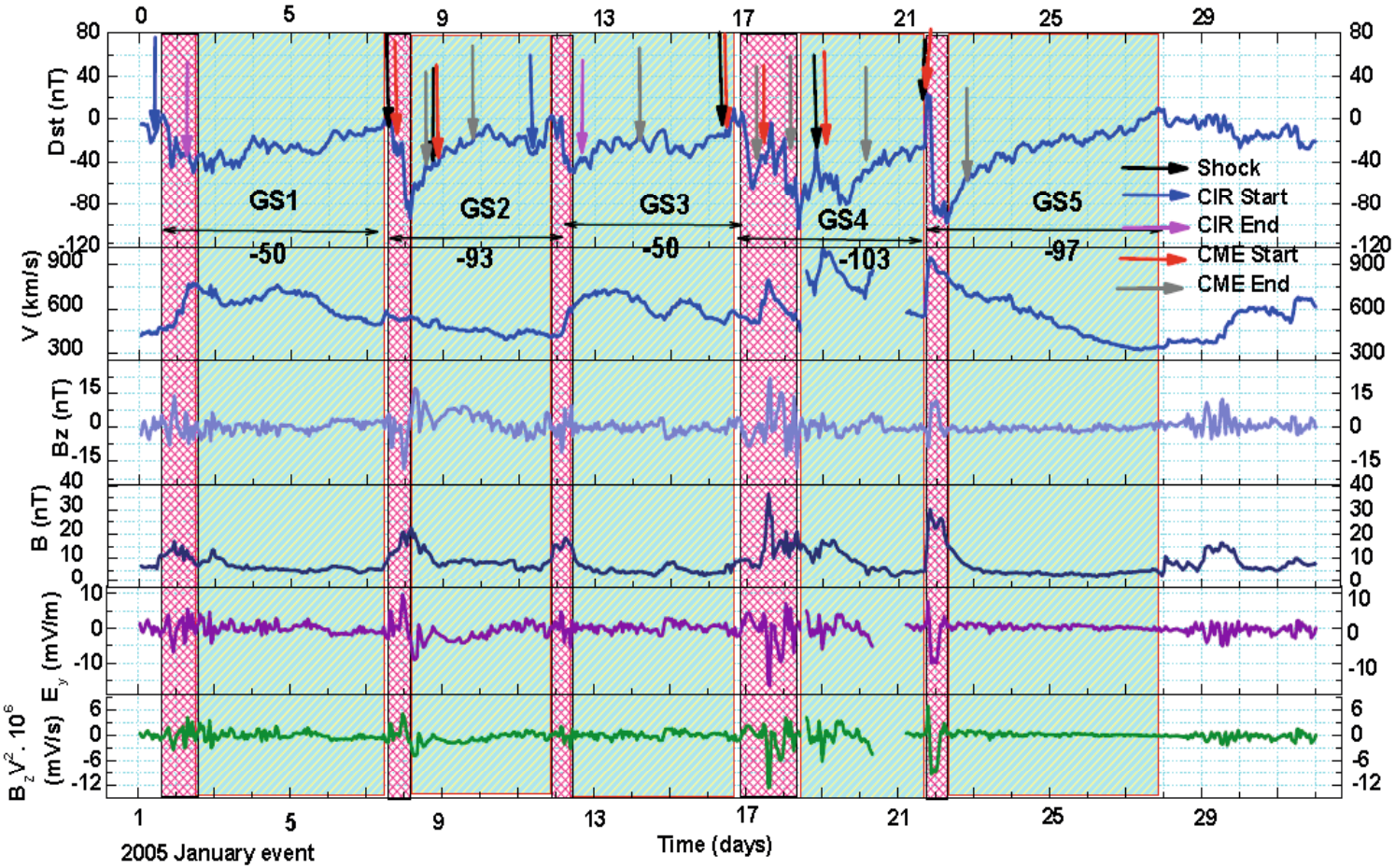

GS1: Dst: -50 nT
Structure : Multi step storm
Solar Source: HSS from CH
Interplanetary structure: CIR
Plasma/field parameter:
B_Z: - 7.8 nT, E_y: 5.54 mV/m

GS2: Dst; -93 nT
Structure : Two step storm
Solar Source: CME
Interplanetary structure:
Sheath, CME
Plasma/field parameter:
B_Z: - 18.2 nT, E_y: 9.65 mV/m

GS3: Dst; -50 nT
Structure : Two step storm
Solar Source: HSS from CH
Interplanetary structure: CIR
Plasma/field parameter:
B_Z: - 10.9 nT, E_y: 4.70 mV/m

GS4: Dst: -103 nT
Structure: Multi step storm
Solar Source: CMEs
Interplanetary structure: Sheath, CME
Plasma/field parameter:
B_Z: - 17.6 nT, E_y: 4.28 mV/m

GS5: Dst: -97 nT
Structure : Single step storm
Solar Source: CME
Interplanetary structure: Sheath, CME
Plasma/field parameter:
B_Z: - 8.5 nT, E_y: 7.71 mV/m

Time variation (hourly data) of Dst (nT), V(km/s), B (nT), its north-south component (B_z) and the product B_zV^2 during April 2001.

GS1: Dst: -50 nT
Structure: Single step storm
Solar Source: CME
Interplanetary structure : Sheath, MC
Plasma/field parameter:
B_Z: - 5.5 nT, E_y: 3.58 mV/m

GS2: Dst: -59 nT
Structure: Single step storm
Solar Source: CME
Interplanetary structure: Sheath, CME
Plasma/ field parameter:
B_Z: - 5.8 nT, E_y: 3.79 mV/m

GS3: Dst: -271 nT
Structure: Two step storm
Solar Source: CME
Interplanetary structure: Sheath, MC
Plasma field parameter:
B_Z: - 20.5 nT, E_y: 14.86 mV/m

GS4: Dst; -77 nT
Structure: Single step storm
Solar Source: CME
Interplanetary structure: Sheath, CME
Plasma/ field parameter:
B_Z: -6.9 nT, E_y: 5.75 mV/m

GS5: Dst: -114 nT
Structure: Single step storm
Solar Source: CME
Interplanetary structure: Sheath, CME
Plasma/ field parameter: B_Z: - 19.6 nT, E_y: 9.72 mV/m

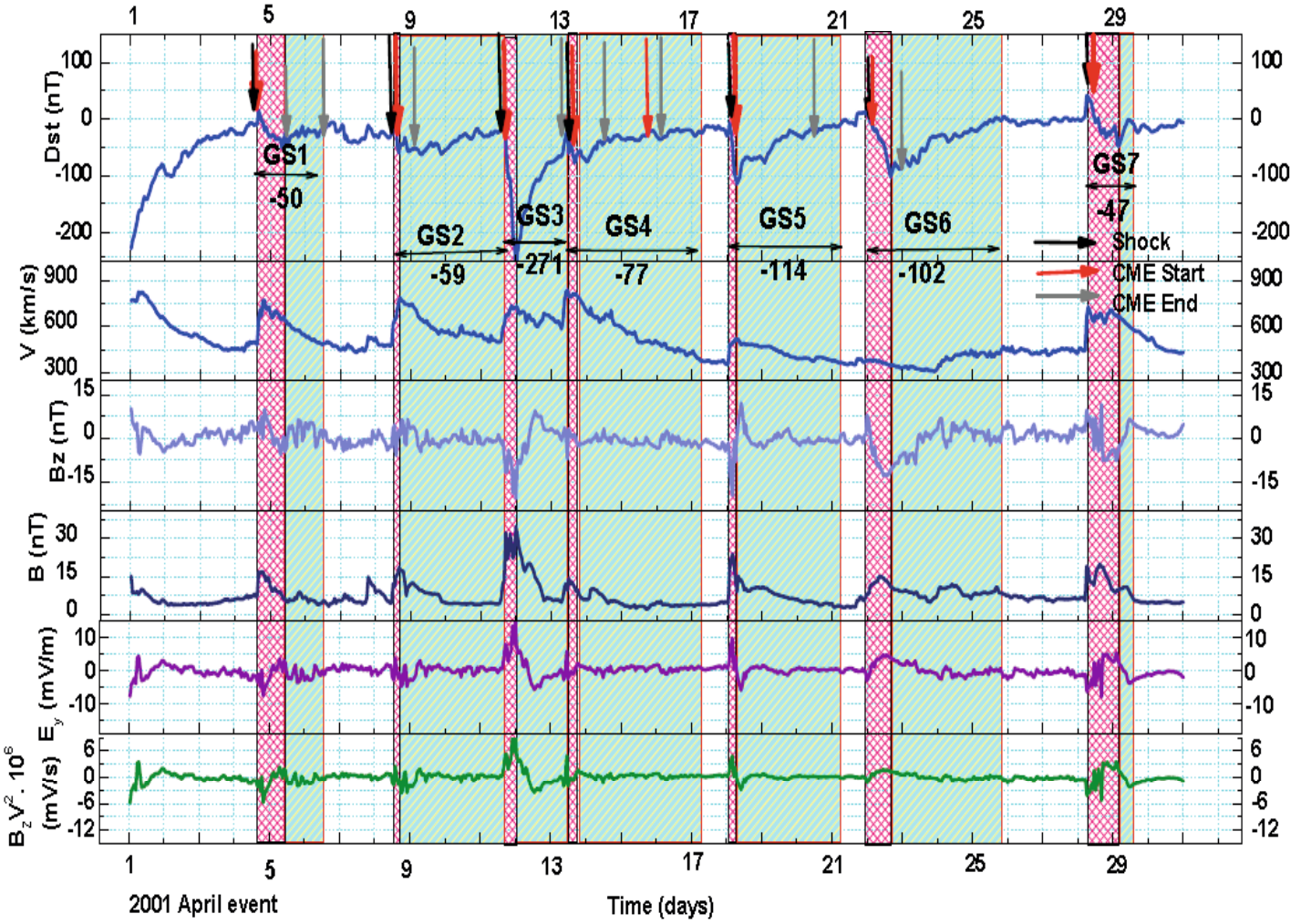

GS6: Dst: -102 nT
Structure: Single step storm
Solar Source: CME
Interplanetary structure: : Sheath, MC
Plasma/ field parameter: B_Z: - 12.8 nT, E_y: 4.65 mV/m

GS7: Dst: -47 nT
Structure: Single step storm
Solar Source: CME
Interplanetary structure: Sheath, MC
Plasma/ field parameter: B_Z: - 7.7 nT, E_y: 4.91 mV/m

Time variation (hourly data) of Dst (nT), V(km/s), B (nT), its north-south component (B_z) and the product B_zV^2 during July 2000.

GS1: Dst: -26 nT
Structure : Small storm
Solar Source: CME
Interplanetary structure: Sheath, MC
Plasma/ field parameter:
B_z: - 7.9 nT, E_y: 1.52 mV/m

GS2: Dst: -43 nT
Structure : Two step storm
Solar Source: CME
Interplanetary structure: Sheath, MC
Plasma/ field parameter:
B_z: - 6.9 nT, E_y: 4.55 mV/m

GS3: Dst: -301 nT
Structure : Two step storm
Solar Source: Sheath, MC
Interplanetary source/structure: CME
Plasma/ field parameter:
B_z: - 45.3 nT, E_y: 47.11 mV/m

GS4: Dst; -93 nT
Structure: Single step storm
Solar Source: CME
Interplanetary structure: Sheath, CME
Plasma /field parameter: B_z: - 7.9 nT, E_y: 4.49 mV/m

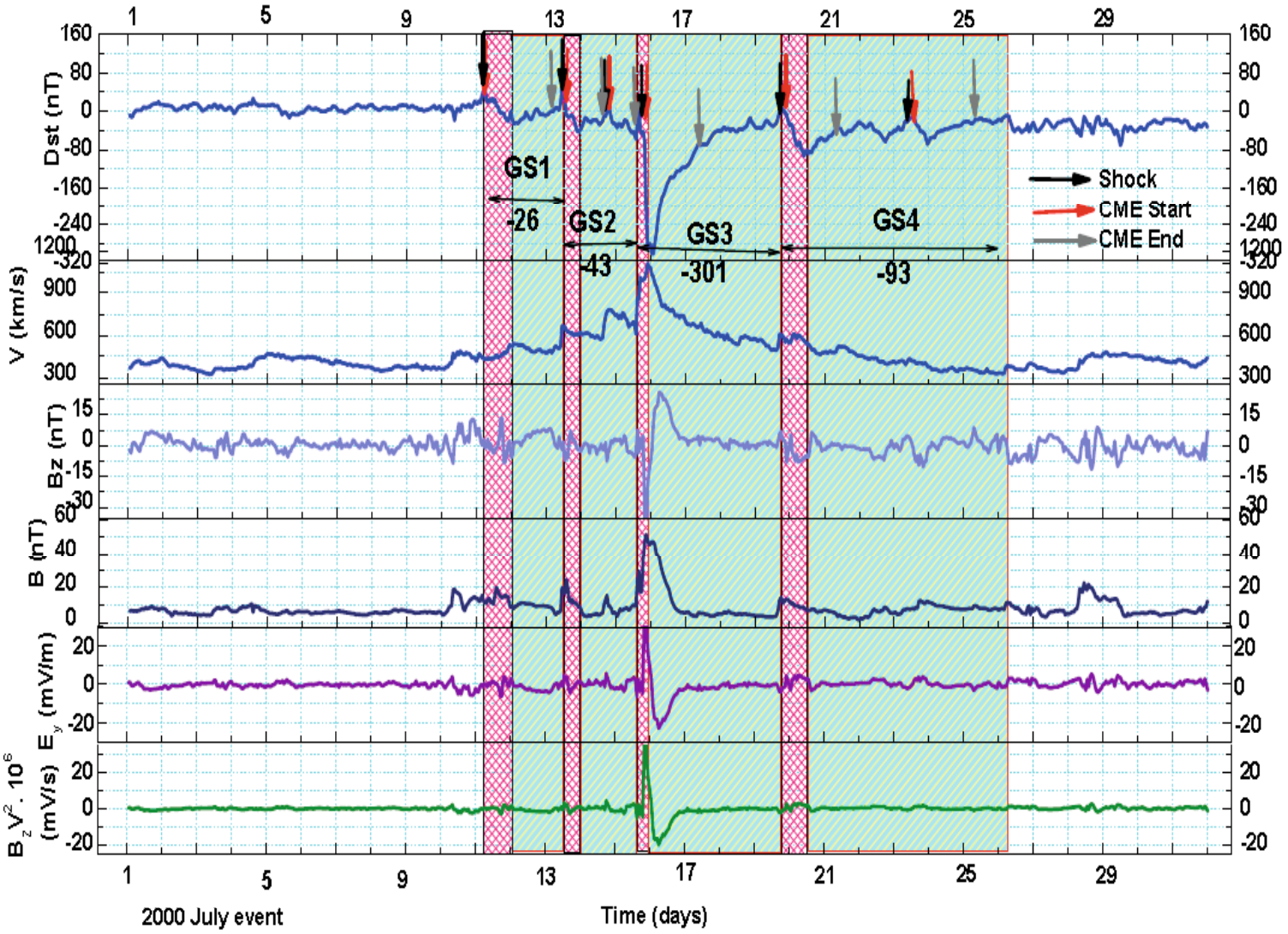

GS, interplanetary plasma/field parameters and responsible structures.

S. No	GS Start time Y/M/D	$(Dst)_{min}$ (nT)	V_{max} (km/s)	$(B_Z)_{min}$ (nT)	B_{max} (nT)	$(E_y)_{max}$ (mV/m)	$(B_ZV^2)_{max}*10^6$ (mV/s)	Structures
1.	2006/12/05	-55	713	-8.9	12.9	4.10	1.89	CIR
2.	2006/12/11	-55	756	-5.1	8.9	3.74	2.75	--
3.	2006/12/14	-162	955	-15.7	17.7	13.56	11.72	SH/MC
4.	2005/01/01	-50	776	-7.8	17.2	5.54	4.26	CIR
5.	2005/01/07	-93	549	-18.2	22.4	9.65	5.11	SH/CME
6.	2005/01/11	-50	729	-10.9	18.3	4.70	2.02	CIR
7.	2005/01/16	-103	798	-17.6	36.8	4.28	2.24	SH/CME
8.	2005/01/21	-97	950	-8.5	30.4	7.71	6.99	SH/CME
9.	2001/04/04	-50	699	-5.5	16.8	3.58	2.33	SH/MC
10.	2001/04/08	-59	782	-5.8	18.5	3.79	2.47	SH/CME
11.	2001/04/11	-271	732	-20.5	34.5	14.86	10.77	SH/MC
12.	2001/04/13	-77	833	-6.9	14.3	5.75	4.79	SH/CME
13.	2001/04/18	-114	519	-19.6	23.8	9.72	4.82	SH/CME
14.	2001/04/21	-102	379	-12.8	15.1	4.65	1.69	SH/MC
15.	2001/04/28	-47	707	-7.7	19.9	4.91	3.38	SH/MC
16.	2000/07/11	-26	541	-7.9	19.8	1.52	0.66	SH/MC
17.	2000/07/13	-43	619	-6.9	24.6	4.55	3.00	SH/MC
18.	2000/07/15	-301	1107	-45.3	51.6	47.11	50.00	SH/MC
19.	2000/07/19	-93	609	-7.9	14.4	4.49	2.82	SH/CME

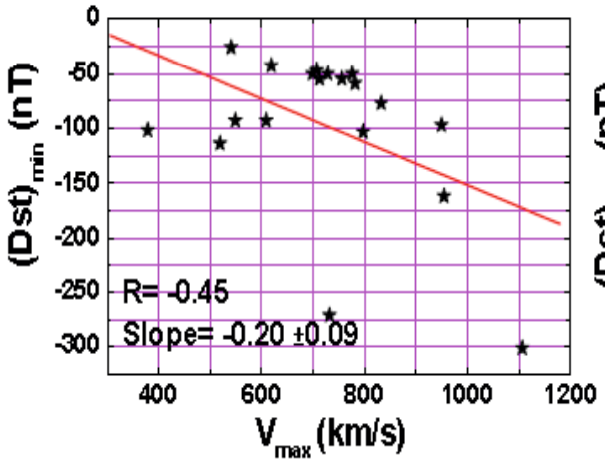

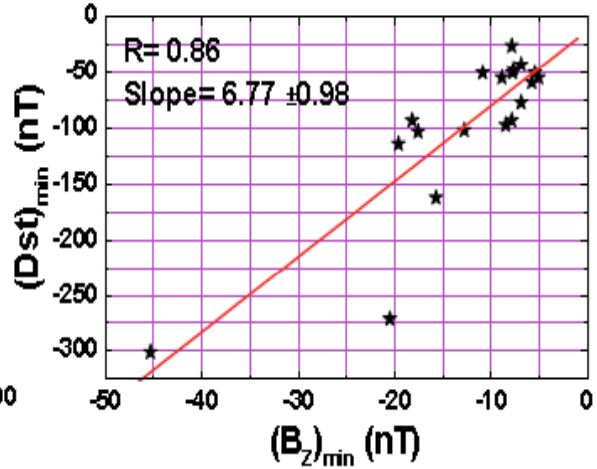

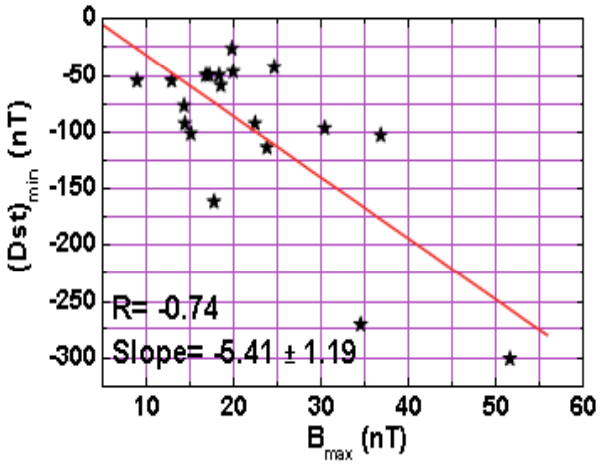

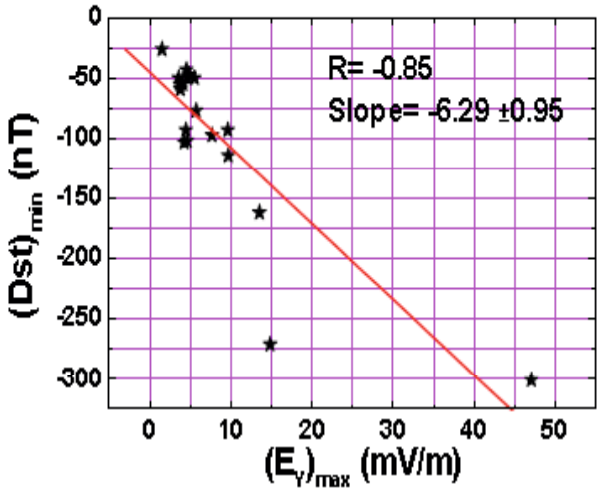

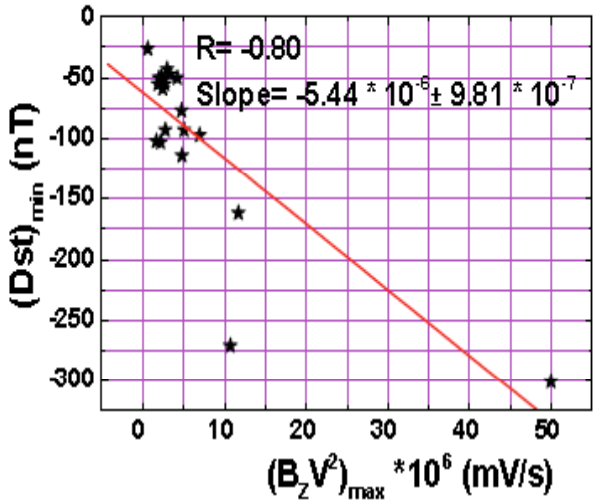

Best correlation are with; -Bz ($\frac{\Delta Dst}{\Delta Bz}$ = 6.77); Ey ($\frac{\Delta Dst}{\Delta Ey}$ = -6.29)

FORBUSH DECREASE: Importance in Space weather research

- The typical effects of a CME, whose interplanetary counterpart is ICME, is to suppress the intensity of the ambient cosmic rays (of galactic origin) in the solar wind-called Forbush decrease.

- Forbush decreases are characterized by rapid reduction (within a few hours) in cosmic-ray intensity followed by a slow recovery typically lasting several days. These FDs are generally associated with shock/sheath/magnetic cloud structures formed due to coronal mass ejections from sun.

- Precursor anisotropies upstream to CME shock, if present, have potential application in space weather forecasting system. The loss-cone precursor anisotropy predicts the arrival of interplanetary shocks and the associated ICMEs.

- Precursor decreases may occur from a 'loss cone' effect, in which particle trajectories trace to the cosmic ray depleted region behind the shock, while precursor increases may result from the particles that have received a small energy boost by reflection from the approaching shock.

- Perpendicular anisotropy is omnipresent during Forbush decreases and the $\overline{B} \times \overline{\nabla} n$ drift flux is the likely cause of perpendicular anisotropy.

- Neutron monitors and muon detectors are located all over the world and accurately detect the intensity variation and anisotropy prior to arrival of the ICME.

- With suitable analysis, ground-based detectors (Neutron monitors and Muon detectors) can yield unique information on conditions in the near-earth interplanetary medium.

- Thus it is possible to use this phenomenon as a warning of a GS.

Time variation (hourly data) of GCR-intensity, solar wind velocity (V), magnetic field vector (F), its slandered deviation (σ_F) along with the product FV and FV^2 during December 2006.

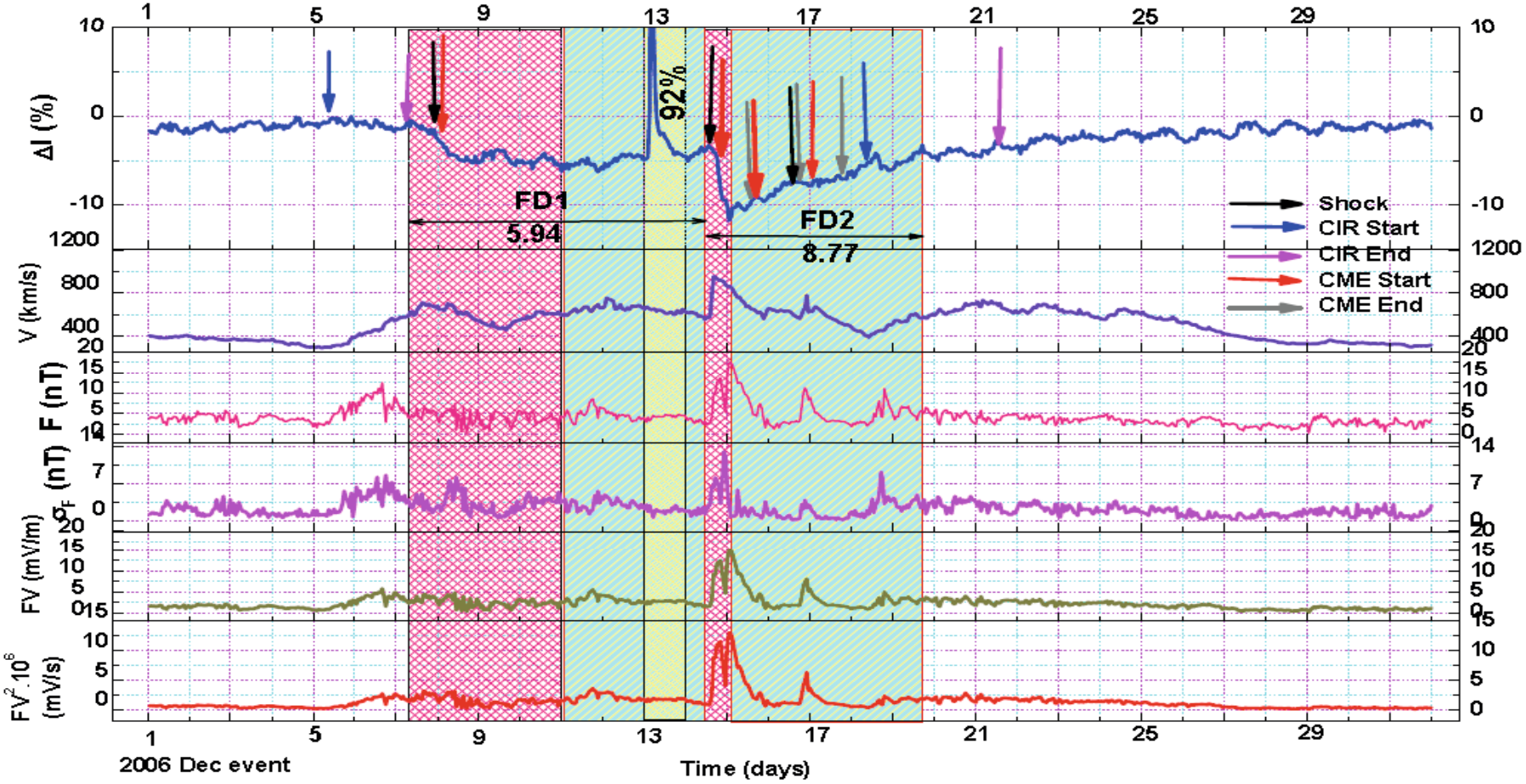

FD1: ΔI: 5.94 %
Structure : Slowly Decreasing
Solar Sources: CH stream, CME
IP structure: CIR, SH/CME
IP plasma/field parameter: Enhanced/Fluctuating
Field F = 12.4 nT, σ_F = 5.9 nT

FD2: ΔI: 8.77 %
Structure : Sharp Decreasing
Solar Sources: CME
IP structure: SH/MC
IP plasma/field parameter: Enhanced/Fluctuating field
F = 17.5 nT, σ_F = 12.1 nT

Energy spectrum of two Forbush decreases observed in December 2006

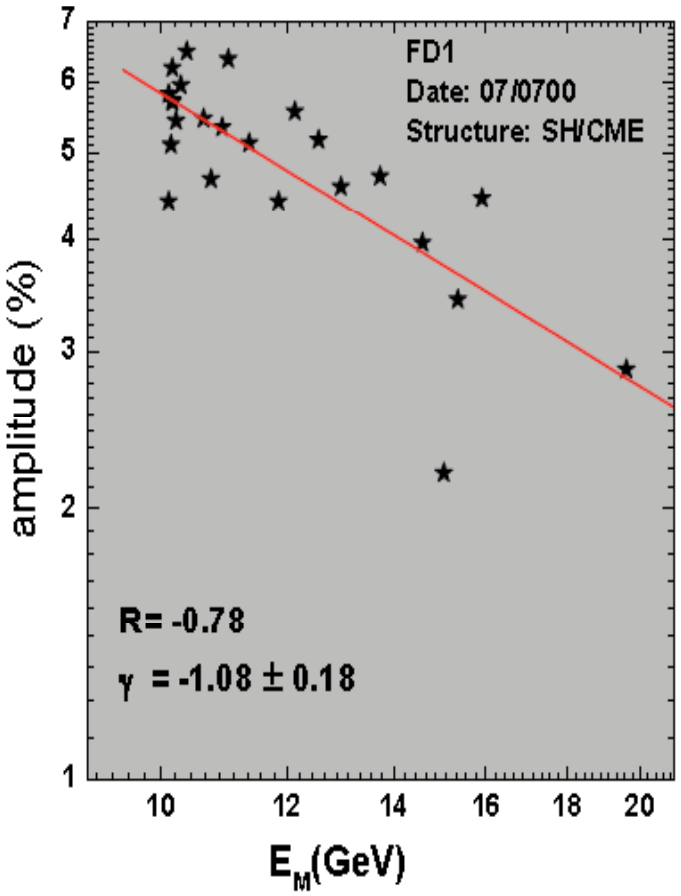

Dec 2006

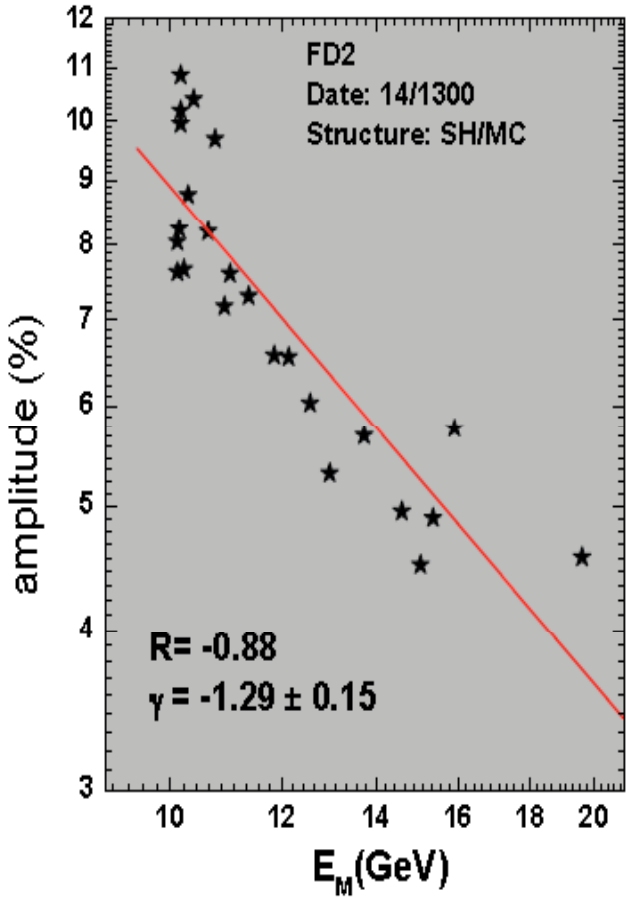

$\Delta I (\%) \alpha E_m^{-\gamma}$

- E_m = *Median Energy (Usoskin et al., 2008)*

$\gamma \rightarrow$ *-1.08 and -1.29*

Time variation (hourly data) of GCR-intensity, solar wind velocity (V), magnetic field vector (F), its slandered deviation (σ_F) along with the product FV and FV^2 during January 2005.

FD1: ΔI: 6.69 %
structure: Slowly Decreasing
Solar Sources: CH stream
IP structure: CIR
IP plasma/field parameter:
Enhanced/Fluctuating field
F = 22.3 nT, σ_F = 8.1 nT

FD2: ΔI: 14.28 %
Structure : Multiple- step
Solar Sources: CMEs
IP structure: SH/CMEs
IP plasma/field parameter:
Enhanced/Fluctuating field
F = 33.7 nT, σ_F = 19.2 nT

FD3: ΔI: 8.18 %
Structure : Sharp Decrease
And fast recovery
Solar Sources: CME
IP structure: SH/CME
IP plasma/field parameter:
Enhanced/Fluctuating field
F = 28.9 nT, σ_F = 24.8 nT

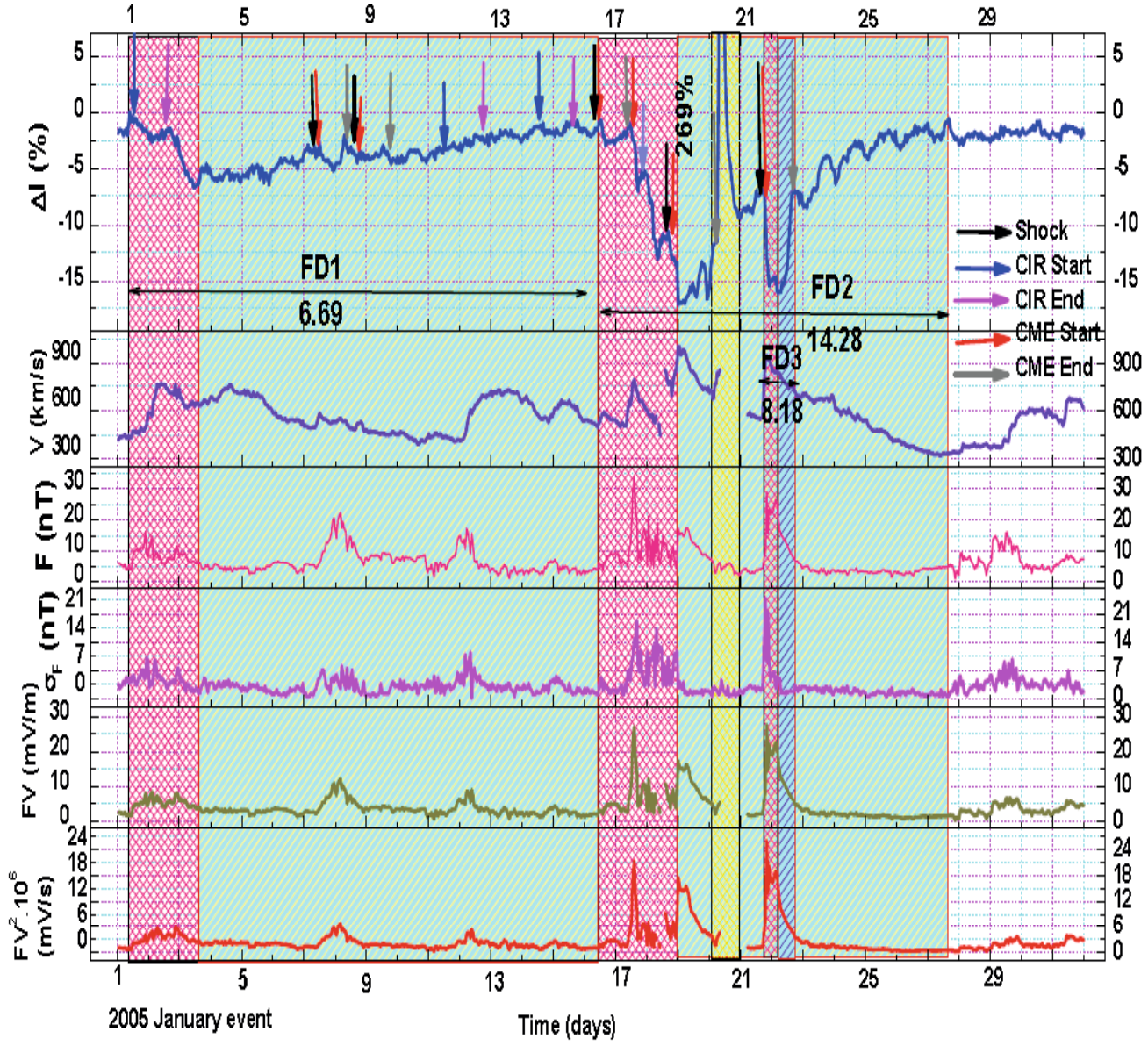

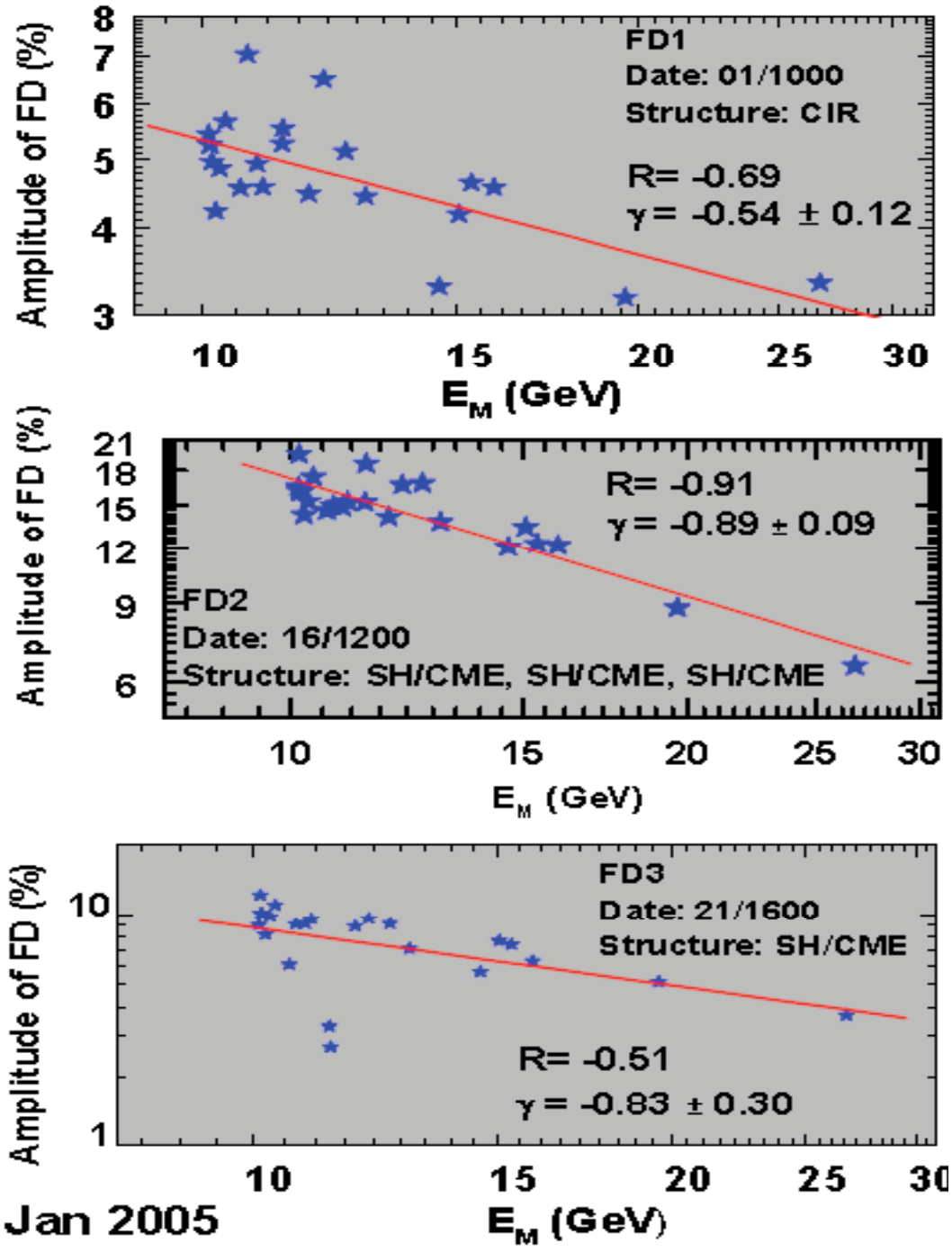

Energy spectrum of three Forbush decreases observed in January 2005

- $\Delta I (\%) \alpha E_m^{-\gamma}$
- *E_m = Median Energy (Usoskin et al., 2008)*
- *γ for three events varies from -0.54 to -0.89*
- *Lower value for CIR associated FD*

Time variation (hourly data) of GCR-intensity, solar wind velocity (V), magnetic field vector (F), its standard deviation (σ_F) along with the product FV and FV^2 during April 2001.

FD1: ΔI: 7.93 %
Structure : Sharp Decreasing
Solar Sources: CME
IP structure: SH/MC
IP plasma/field parameter:
Enhanced/Fluctuating field
F = 15.2 nT, σ_F = 10.1 nT

FD2: ΔI: 7.63 %
Structure: Slowly Decreasing
Solar Sources: CME
IP structure: SH/CME
IP plasma/field parameter:
Enhanced field/Fluctuating
F = 18.4 nT, σ_F = 10.8 nT

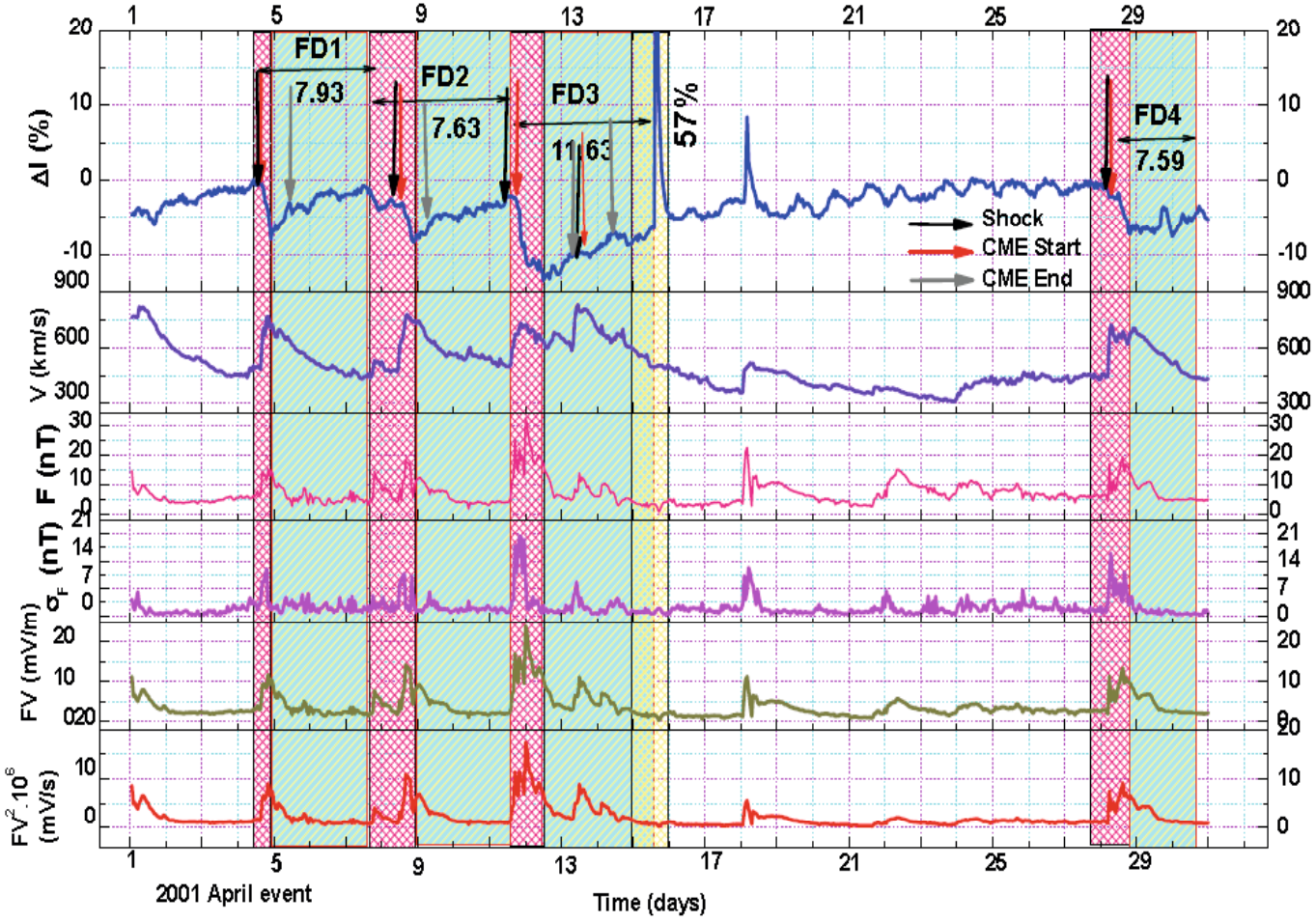

FD3: ΔI: 11.63 %
Structure: Sharp Decreasing
Solar Sources: CMEMC
IP plasma/field parameter:
Enhanced/Fluctuating field F = 25.4 nT, σ_F = 20.3 nT

FD4: ΔI: 7.59 %
Structure: Sharp Decreasing
Solar Sources: CME
IP structure: SH/MC
IP plasma/field parameter: Enhanced/Fluctuating field F = 17.2 nT,
σ_F = 15.9 nT

Energy spectrum of four Forbush decreases observed in April 2001

γ → -0.49 to -1.01

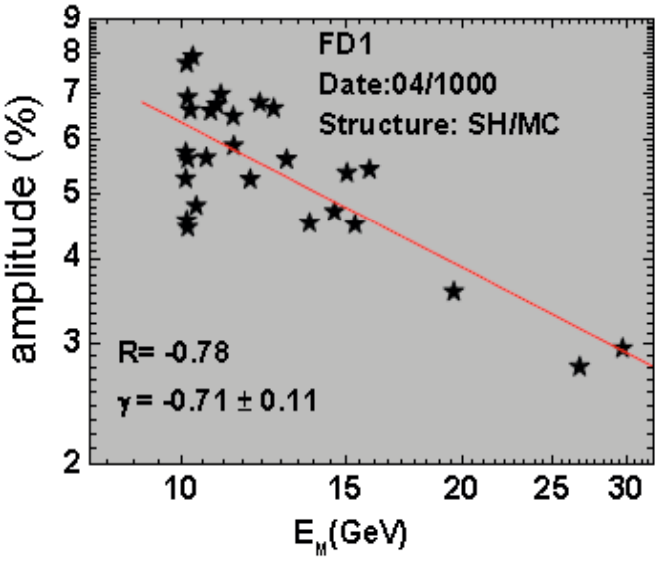

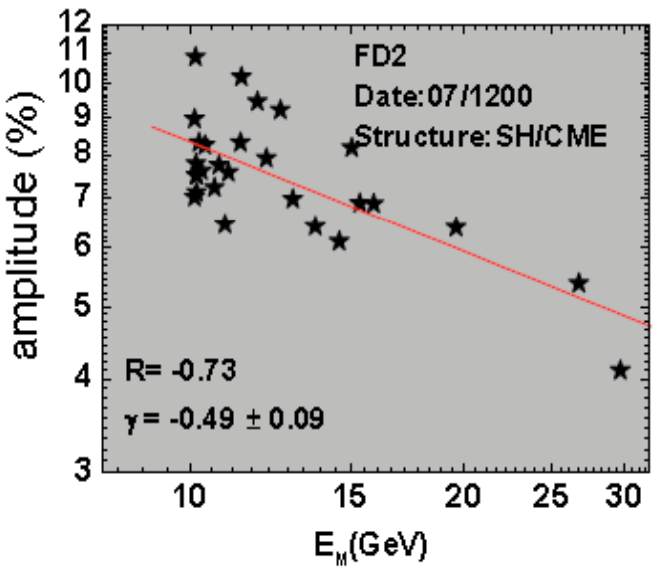

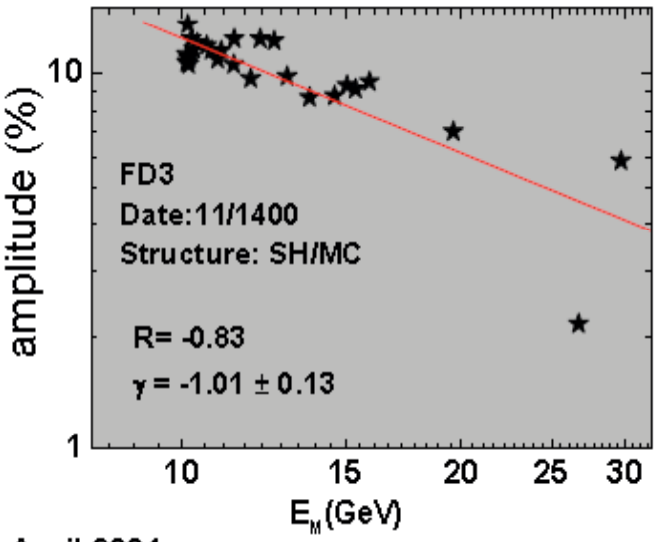

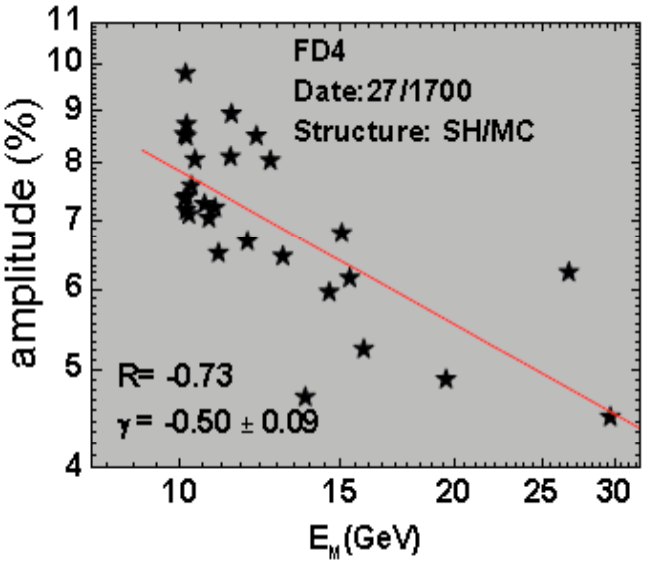

April 2001

Time variation (hourly data) of GCR-intensity, solar wind velocity (V), magnetic field vector (F), its slandered deviation (σ_F) along with the product FV and FV^2 during July 2000.

FD1: ΔI: 4.81 %
Structure : Slowly Decreasin
Solar Sources: CME
IP structure: SH/MC
IP plasma/field parameter:
Enhanced/Fluctuating field
F = 19.2 nT, σ_F = 10.4 nT

FD2: ΔI: 8.96 %
Structure : Sharp Decreasing
Solar Sources: CME
IP structure: SH/MC
IP plasma/field parameter:
Enhanced/Fluctuating field,
F = 22.6 nT, σ_F = 10.4 nT

FD3: ΔI: 10.48 %
Structure : Sharp Decreasing
Solar Sources: CME
IP structure: SH/MC
IP plasma/field parameter:
Enhanced/Fluctuating field
F = 49.4 nT, σ_F = 35.6 nT

FD4: ΔI: 2.46 %
Structure : Sharp Decreasing
Solar Sources: CME
IP structure: SH/CME
IP plasma/field parameter:
Enhanced/Fluctuating field F = 14.2 nT, σ_F = 4.3 nT

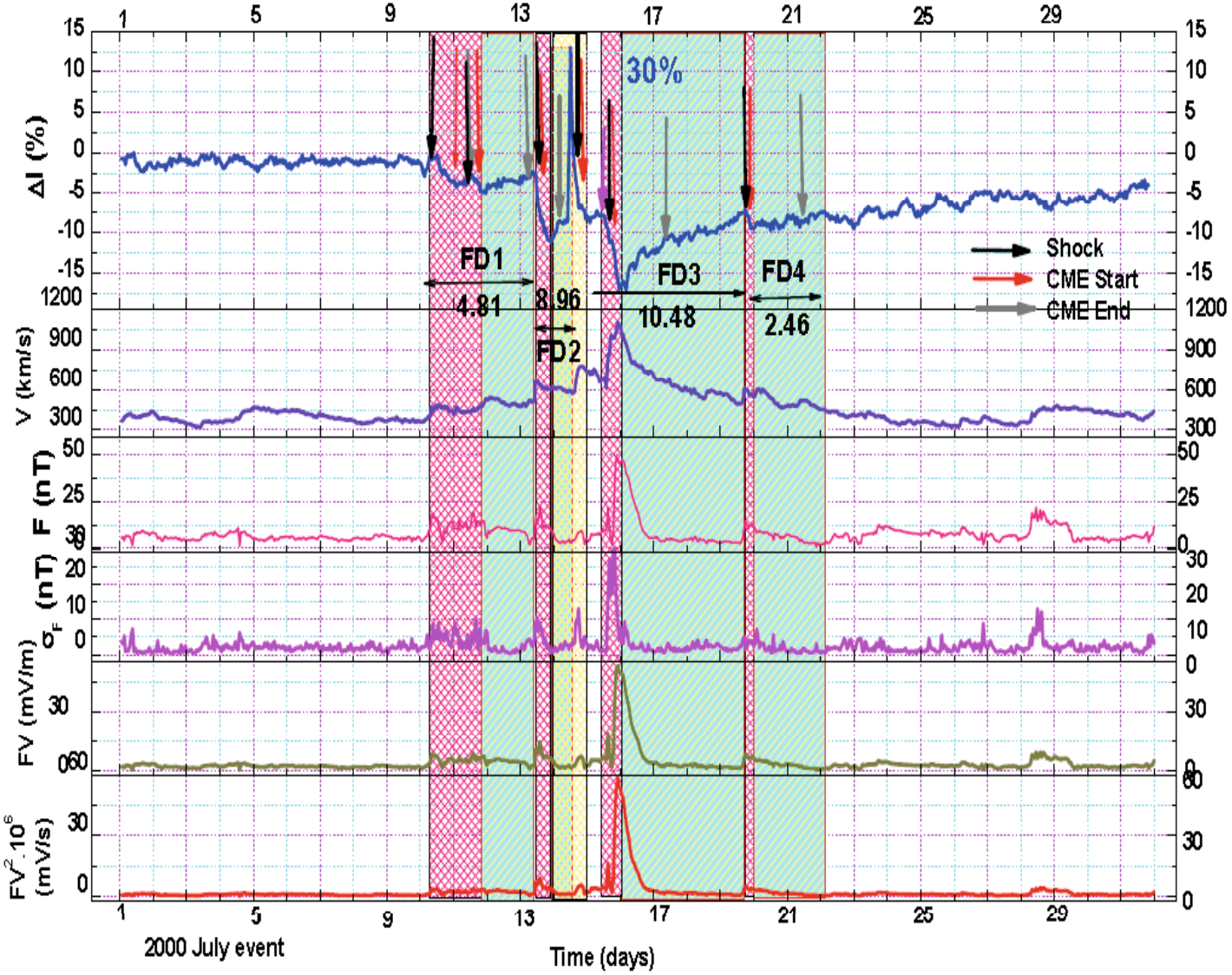

Energy spectrum of four Forbush decreases observed in July 2000

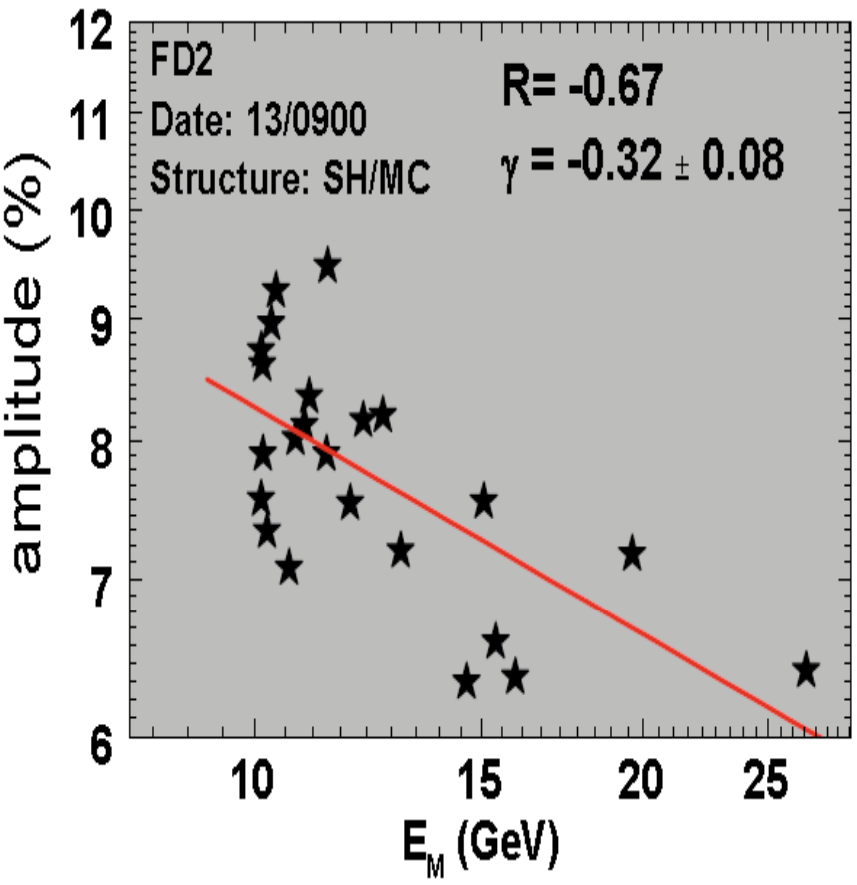

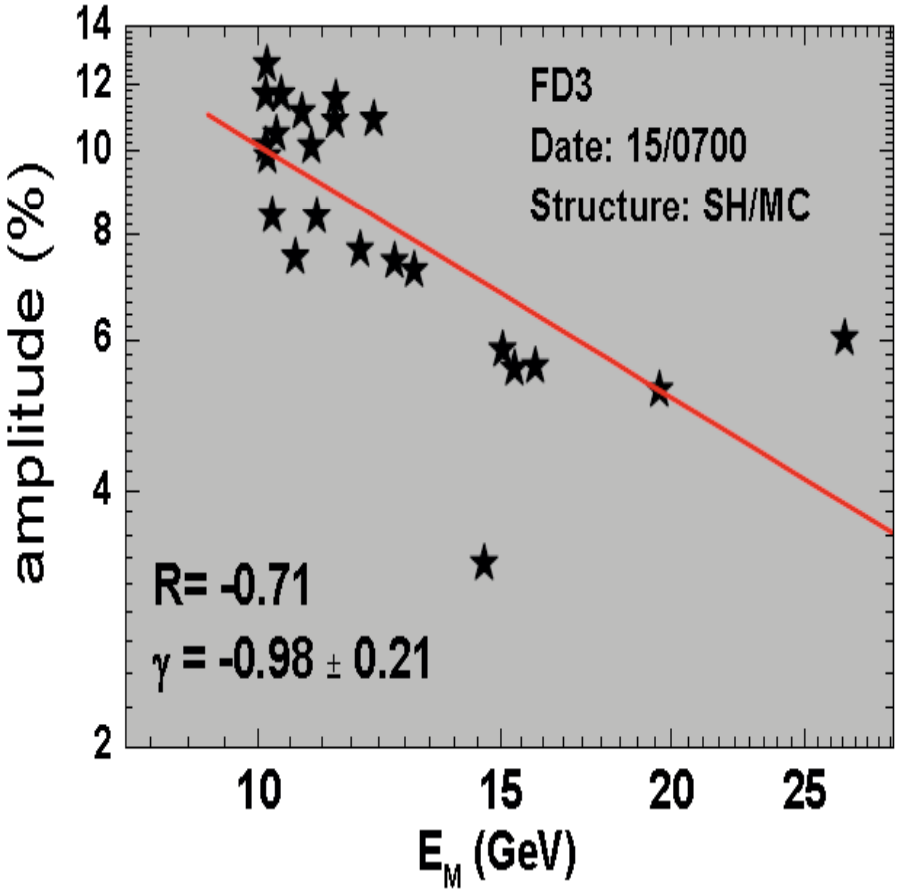

July 2000

FDs, Interplanetary plasma/field parameters, responsible interplanetary structures and energy exponents

FD Start time Y/M/D	Amplitude FD (%)	V_{max} (km/s)	F_{max} (nT)	$(\sigma_F)_{max}$ (nT)	$(FV)_{max}$ (mV/m)	$(FV^2)_{max}$ *10^6 (mV/s)	Responsible Structures	Mach Number	Energy Exponent (γ)
2006/12/07	5.94	713	12.4	5.9	5.77	2.69	CIR, SH/CME	4.33	-1.08 ± 0.18
2006/12/14	8.77	955	17.5	12.1	15.03	12.99	SH/MC	8.53	-1.29 ± 0.15
2005/01/01	6.69	549	22.3	8.1	7.2	3.54	CIR	--	-0.54 ± 0.12
2005/01/16	14.28	798	33.7	19.2	26.89	21.46	SH/CME, SH/CME, SH/CME	1.37	-0.89 ± 0.09
2005/01/21	8.18	950	28.9	24.8	27.45	26.08	SH/CME	7.50	-0.83 ± 0.30
2001/04/04	7.93	768	15.2	10.1	11.67	8.97	SH/MC	5.75	-0.71 ± 0.11
2001/04/07	7.63	782	18.4	10.8	14.15	10.88	SH/CME	3.48	-0.49 ± 0.09
2001/04/11	11.63	833	25.4	20.3	24.00	17.40	SH/MC	2.40	-1.01 ± 0.13
2001/04/27	7.59	724	17.2	15.9	11.35	9.18	SH/MC	5.05	-0.50 ± 0.09
2000/07/10	4.81	541	19.2	10.4	8.79	4.03	SH/CME, SH/MC	1.84	--
2000/07/13	8.96	667	22.6	10.4	14.35	9.11	SH/MC	2.03	-0.32 ± 0.08
2000/07/15	10.48	1010	49.4	35.6	52.58	58.21	SH/MC	7.50	-0.98 ± 0.21
2000/07/19	2.46	605	14.2	4.3	8.48	5.06	SH/CME	2.97	--

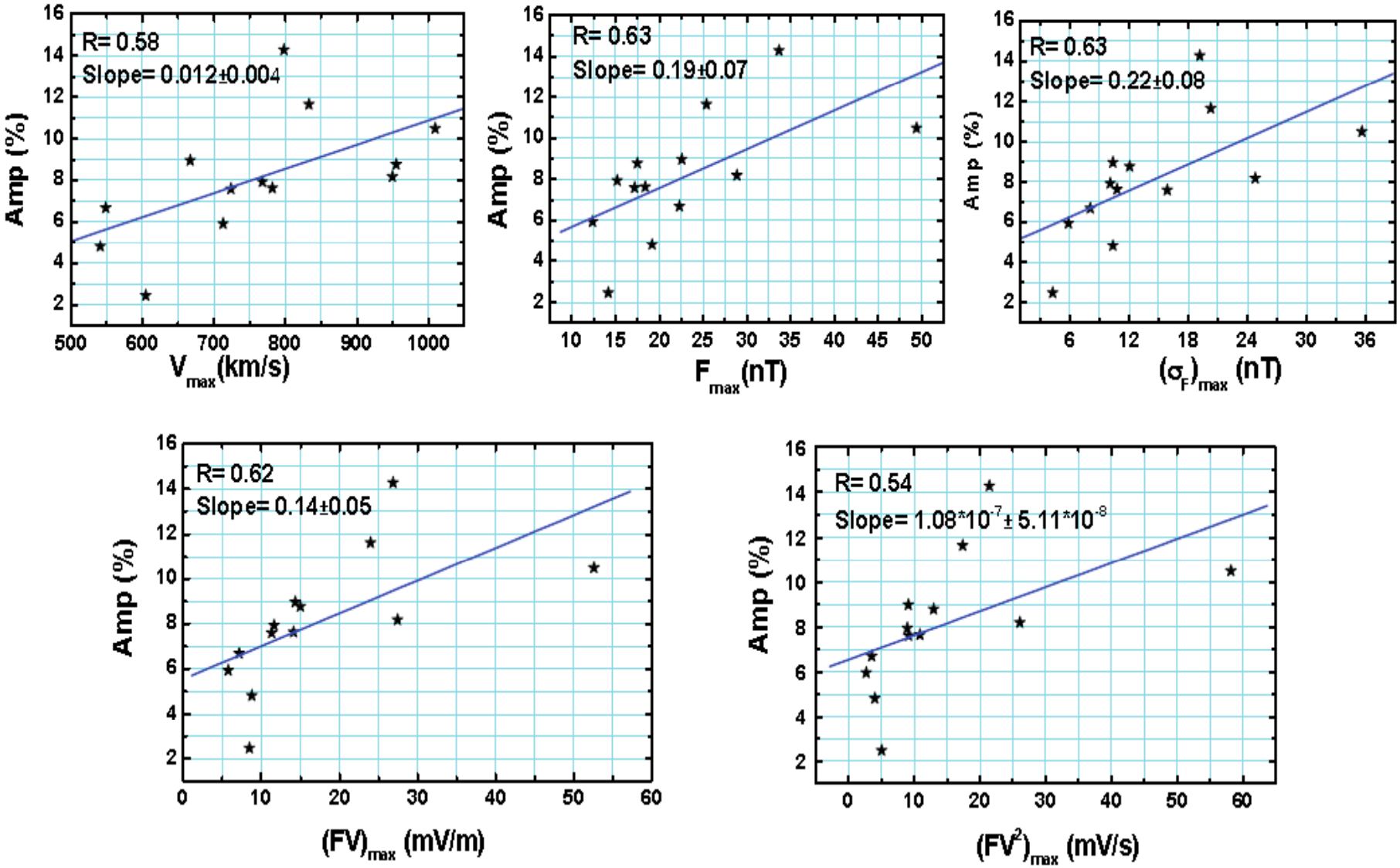

Enhanced and turbulent Magnetic field is best correlated with FD amplitude ($\frac{\Delta I}{\Delta F}$ = 0.2% /nT)

Scatter plots FD amplitude, interplanetary parameters and mach number with Energy exponent

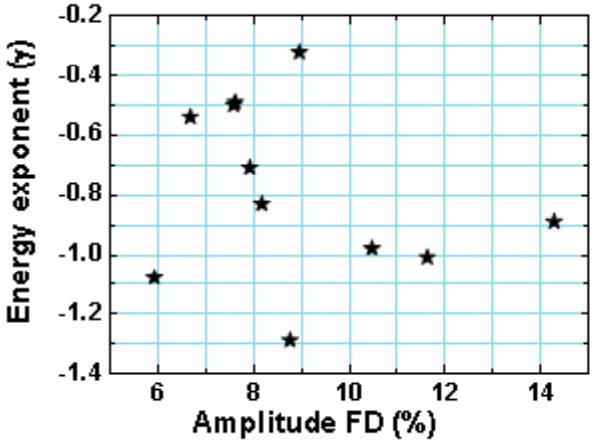

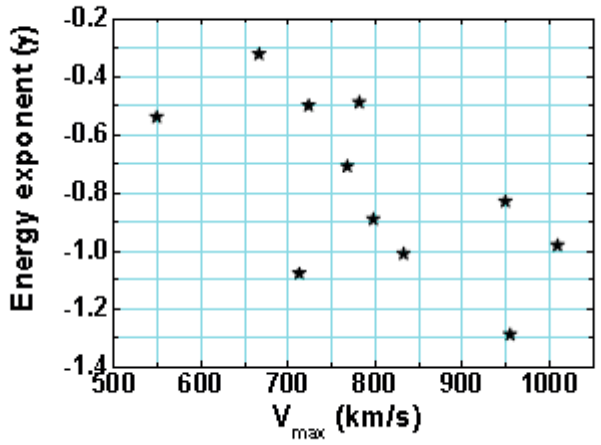

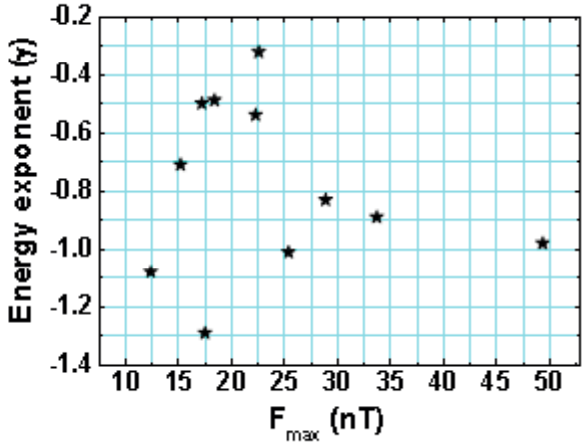

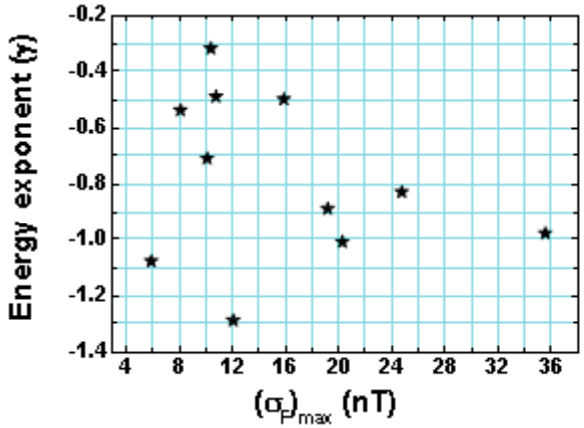

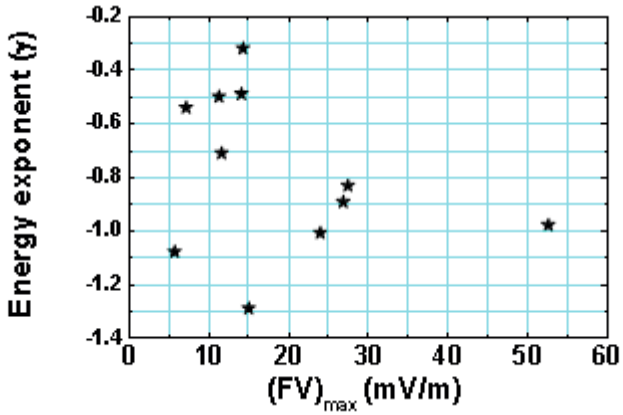

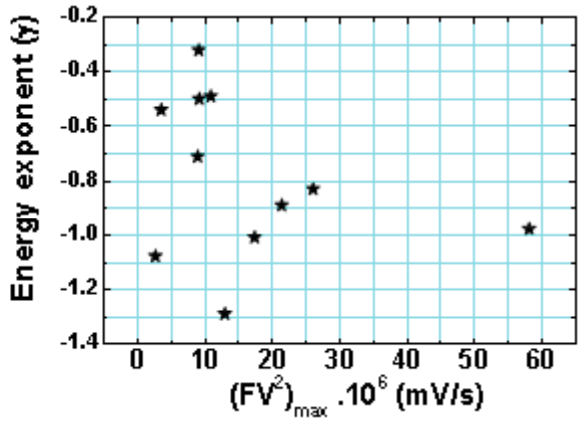

Energy exponent (γ) deos not appear to depend on;

- The amplitude of the decrease
- Speed of the responsible structure
- Field enhancement during its passage
- Standard deviation in field vector
- The mach number of associated shock

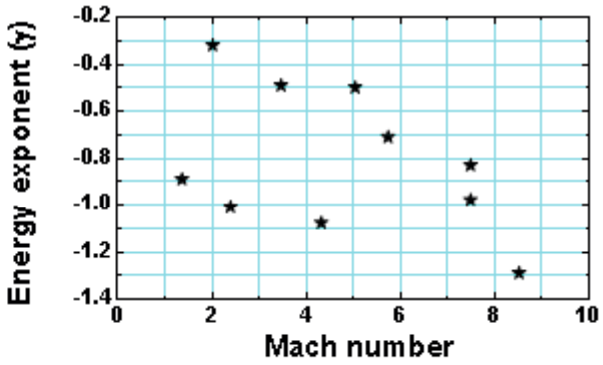

Expanded Figure Dec 2006

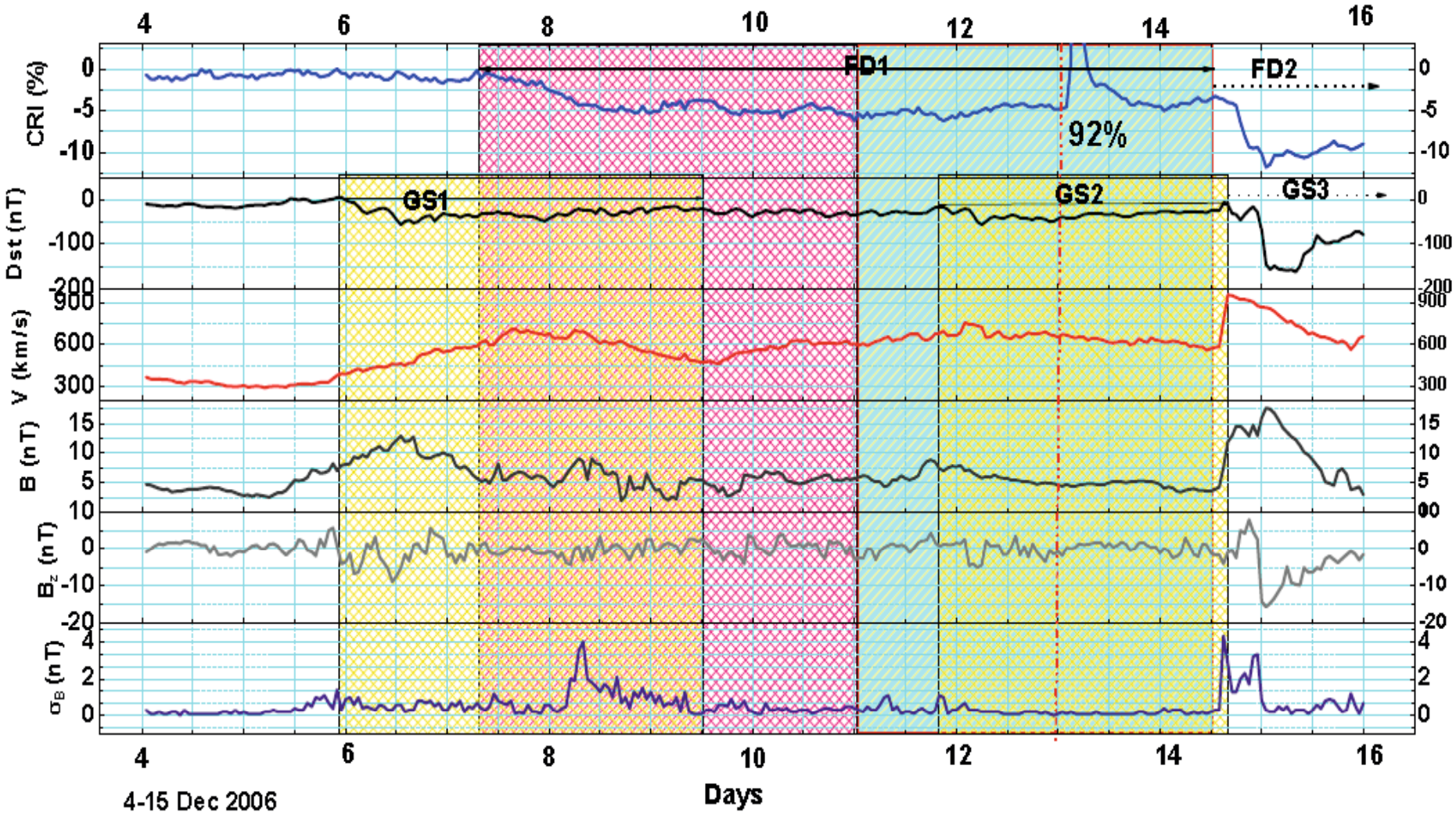

- GLE during recovery phase of FD
- GLE during magnetically quiet period
- FD2 starts earlier than GS3
- Pre-decrease before FD2

Expanded Figure Dec 2006 - continued

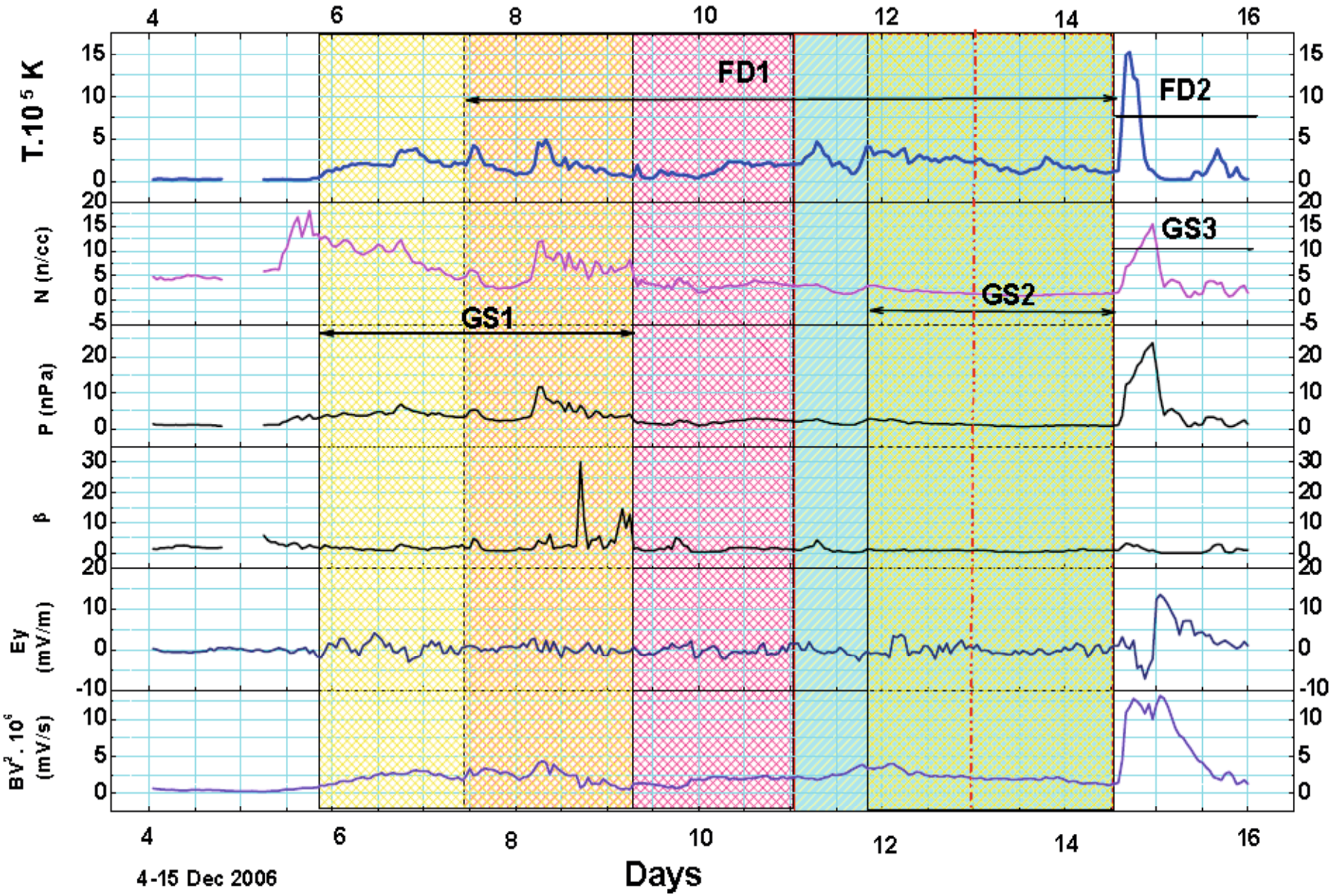

Expanded Figure Jan 2005

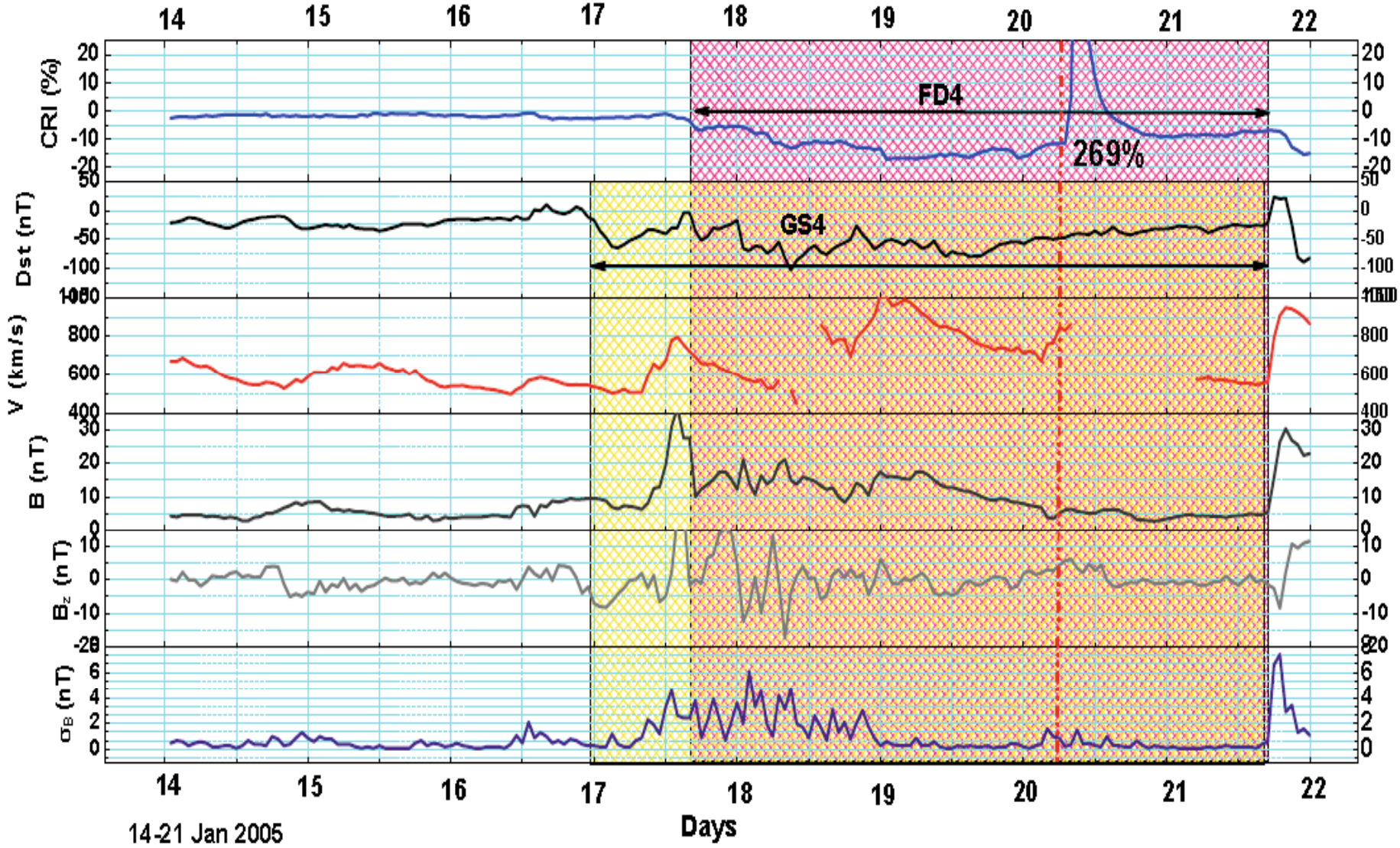

- GLE during recovery phase of FD
- GLE during low B and σ_B condition
- GS4 starts but no FD

Expanded Figure Jan 2005 - continued

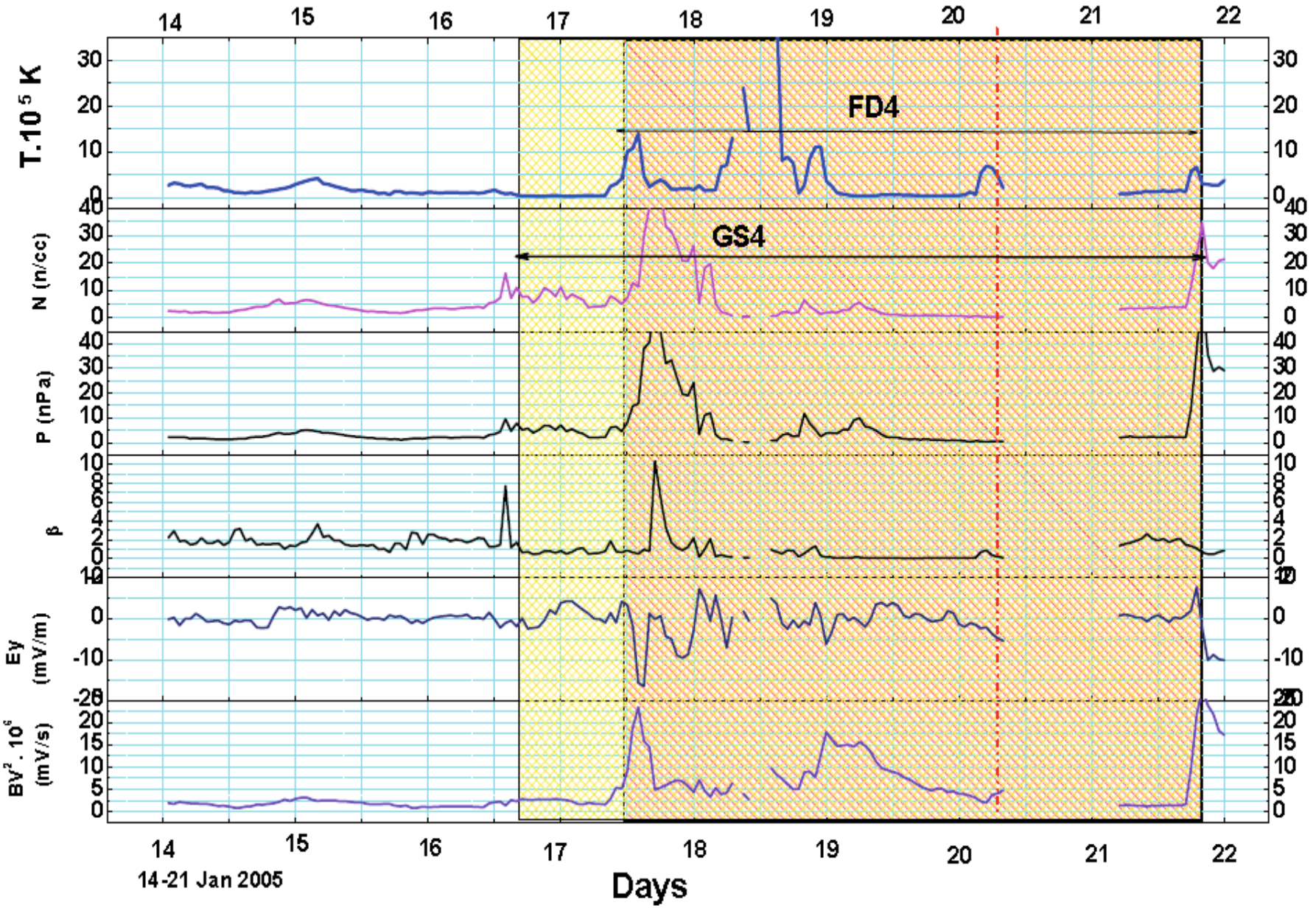

Expanded Figure April 2001

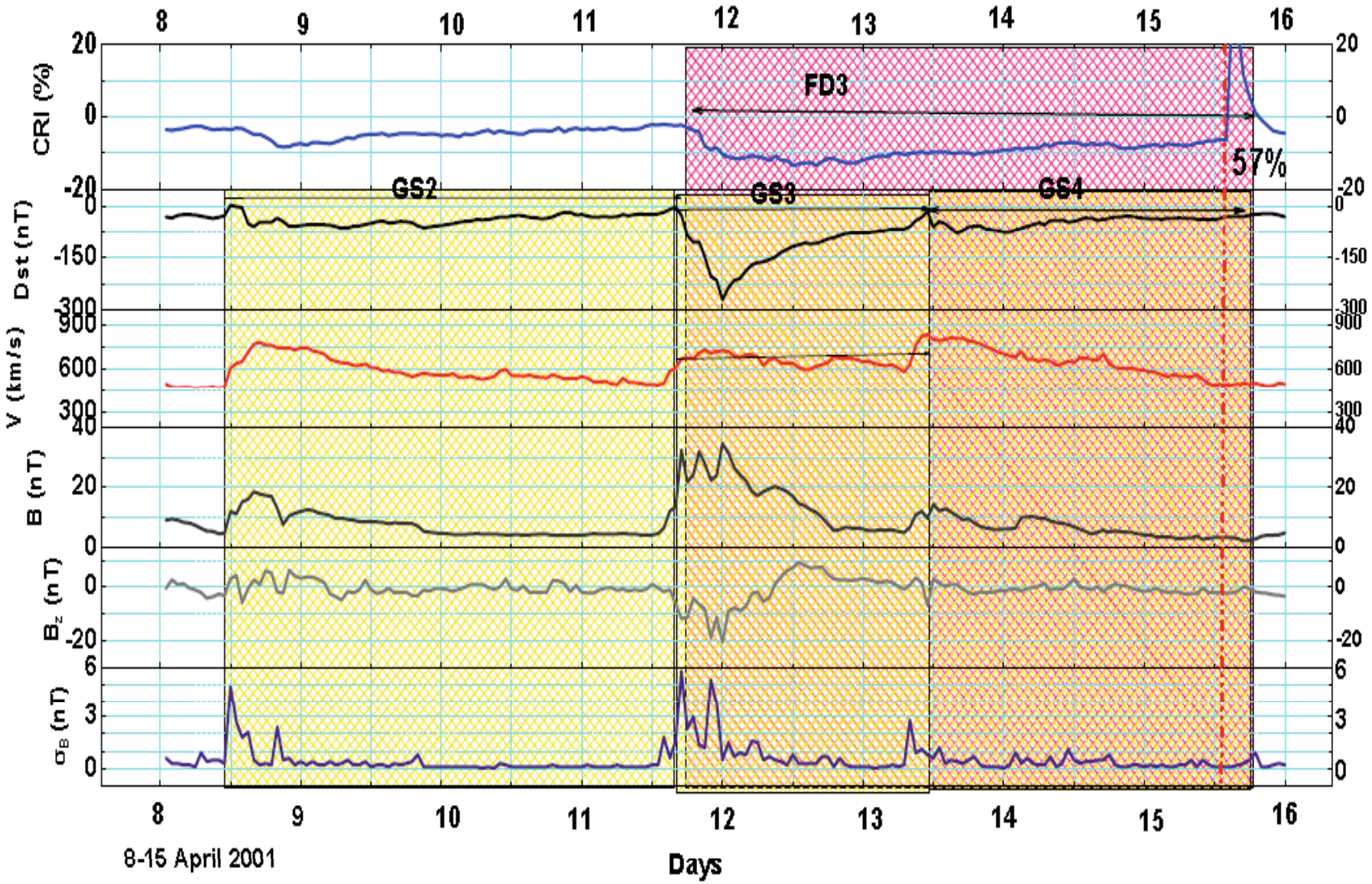

➢GLE during recovery phase of FD

Expanded Figure April 2001 - continued

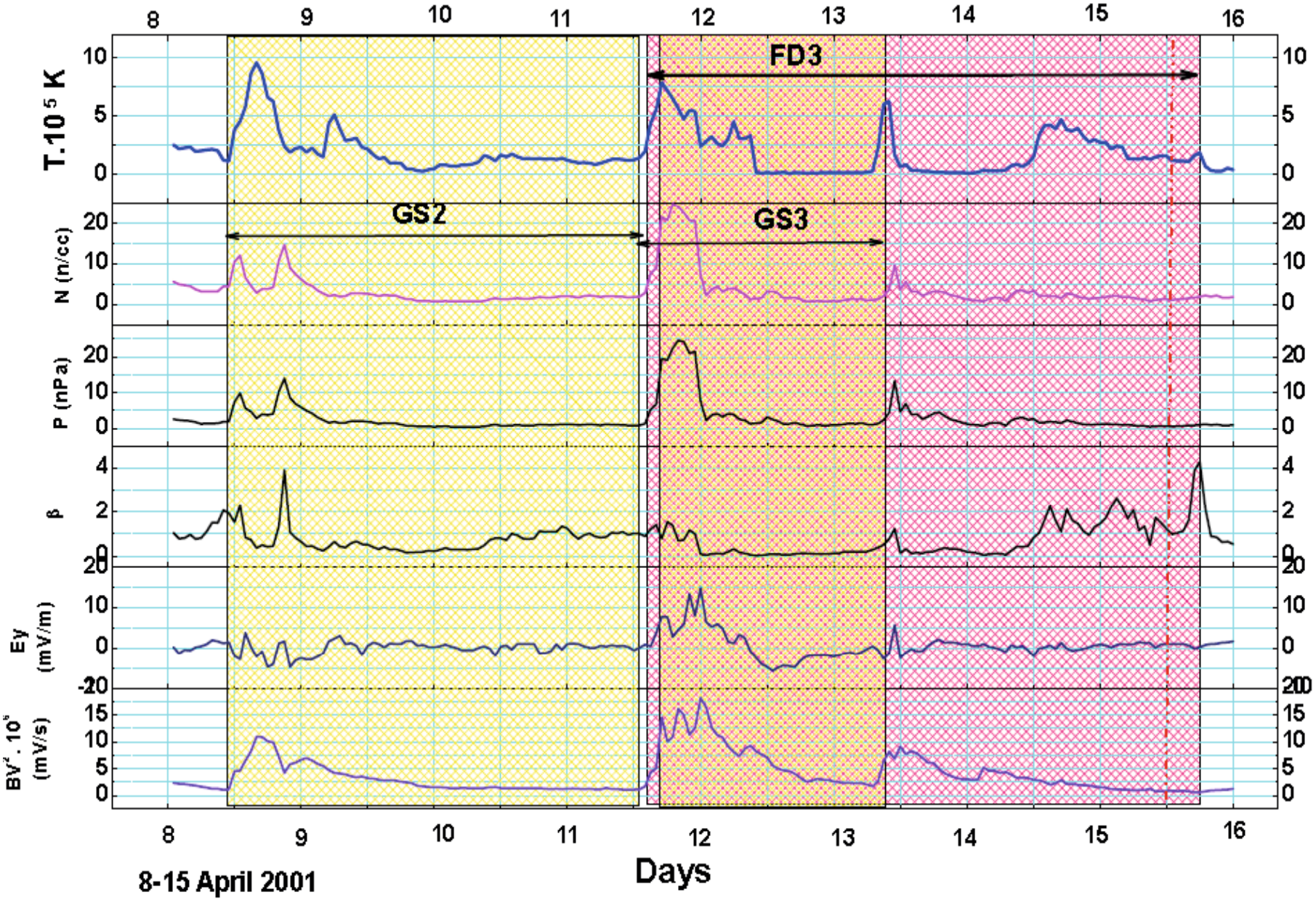

Expanded Figure July 2000

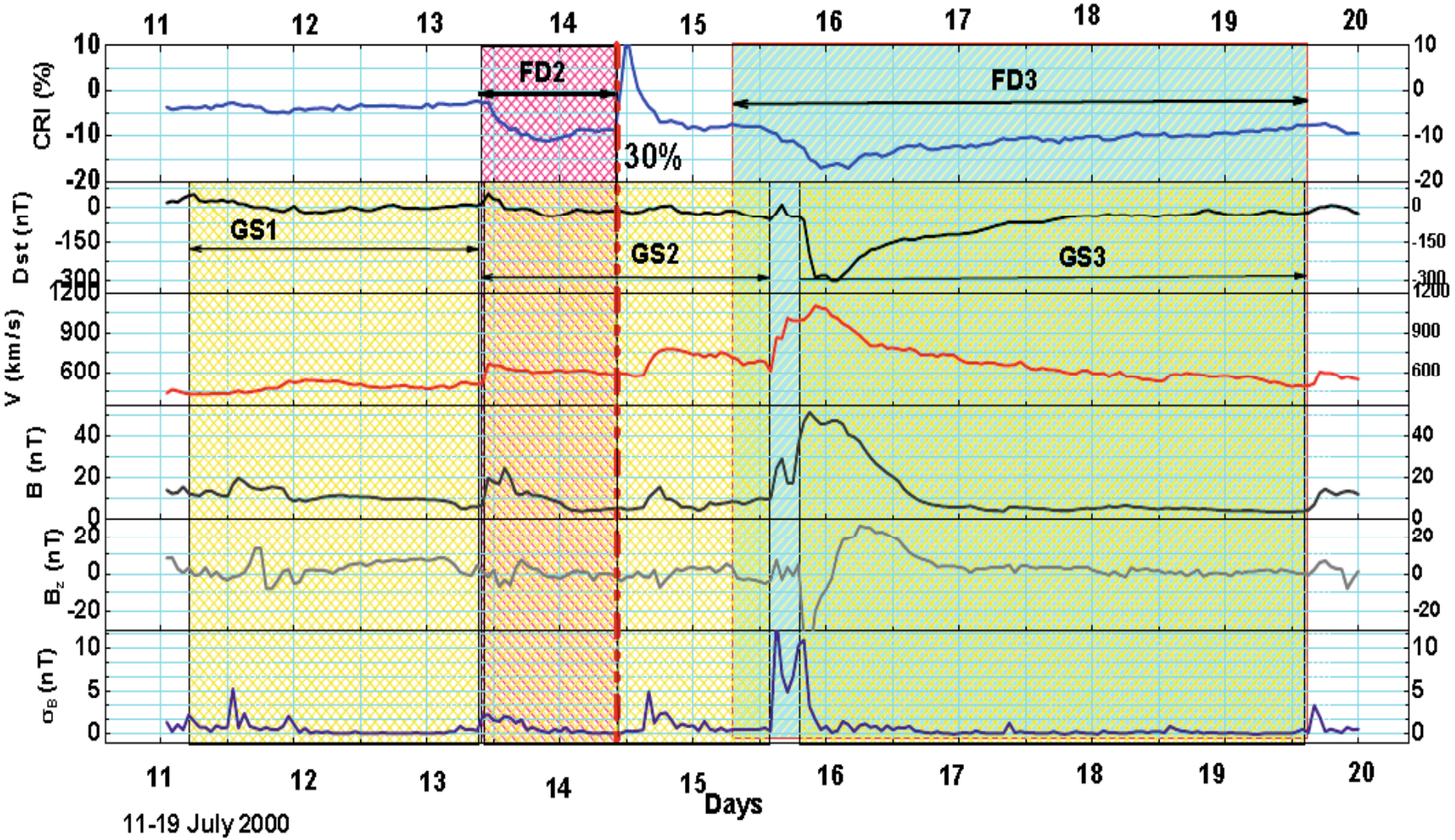

- GLE during recovery phase of FD
- GLE during low B and σ_B condition
- FD3 starts earlier than GS3

Expanded Figure July 2000 - continued

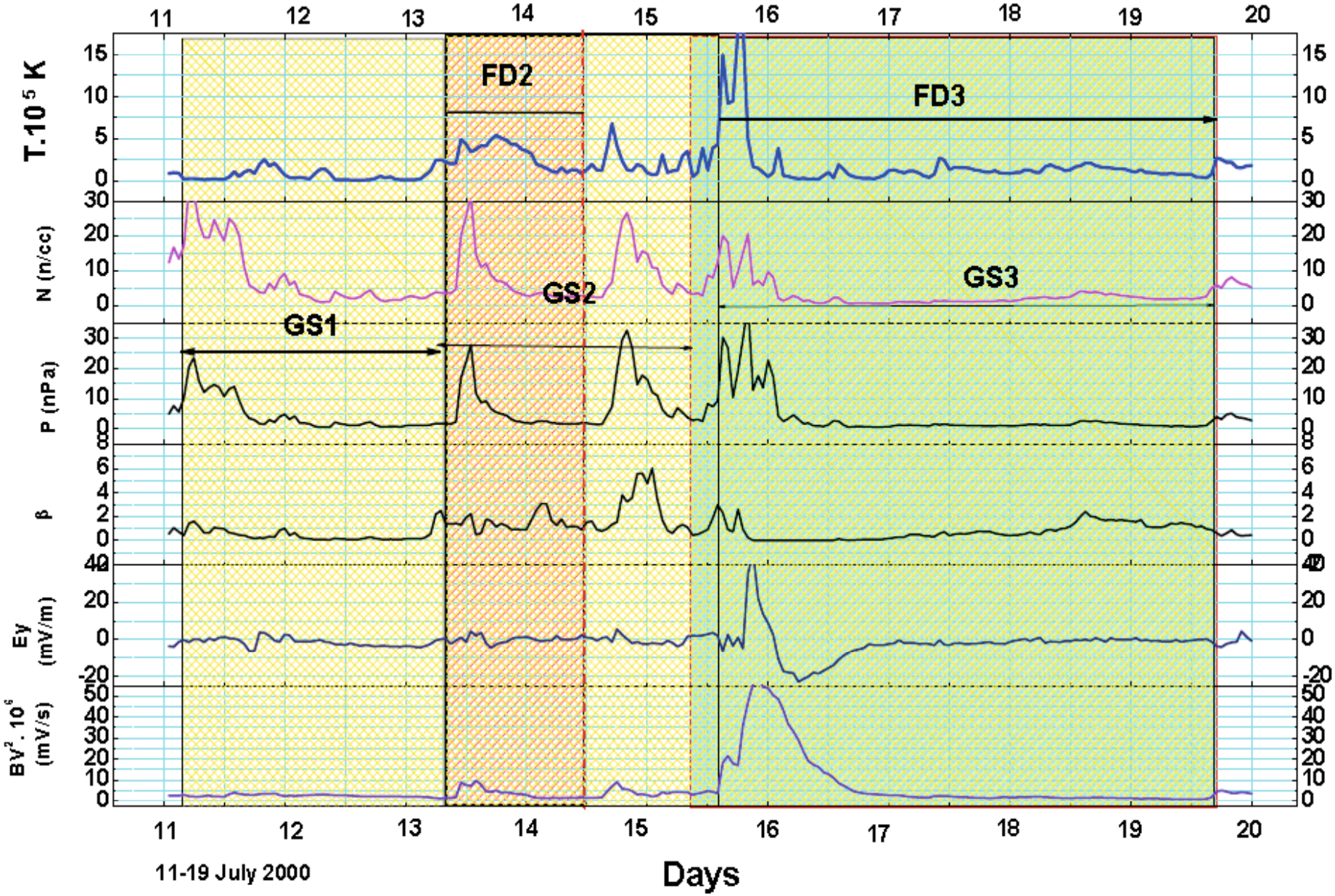

Ground Level Enhancements (GLEs)

- GLEs are observed by neutron monitors when the energy of accelerated particles in the flare or in interplanetary space exceeds the atmospheric threshold and geomagnetic cut off rigidity.

The large Solar Energetic Particle (SEP) fluxes affect the space weather in two main aspects.

1. The relativistic proton fluxes can lead to dangerous radiation doses to unprotected technical systems and astronauts.

2. The fluxes of energetic protons impact the earth's middle atmosphere polar caps by producing enhanced ionizations, excitations, dissociation of atmospheric atoms and molecules. That causes e.g. ozone depletion in the polar upper atmosphere.

Forecasting the large SEPs (GLEs) is still not possible, for two main reasons

1. We have not yet identified unique signatures for the driving flare that would indicate an imminent explosion and its probable onset time, location and strength - Efforts should continue in this direction.

2. The size of SEP fluxes (GLEs) is highly variable and appears to be loosely related to the strength of the flare - Efforts should continue to identify the solar parameter that better relates the size (amplitude) of GLE.

- **Currently there are no known methods to predict, from initial solar observations, if specific solar activity will produce a GLE. However, there is a hope, and efforts are in progress, to use neutron monitors observations for their predictions - a new tool for early warning of radiation storm**

- **The acceleration of particles to such high energies on time scales of seconds to minutes as well as their propagation through space is still not well understood - the research in this area should be actively pursued.**

- Since only a few percent of solar eruptions result in significant events at 1AU, understanding the solar and interplanetary conditions in which these GLEs are generated in vital and attention should continue to be focused to understand them.
- It is important to search for primary characteristics that make a CME or flare produce GLEs.
- It is important to identify the condition when acceleration is most efficient.
- How can we characterize and predict SEPs and their impact in near earth space and atmosphere?

Four different GLEs observed at Oulu NM (per minute resolution), Timings of Flare, CME and GLE are also shown

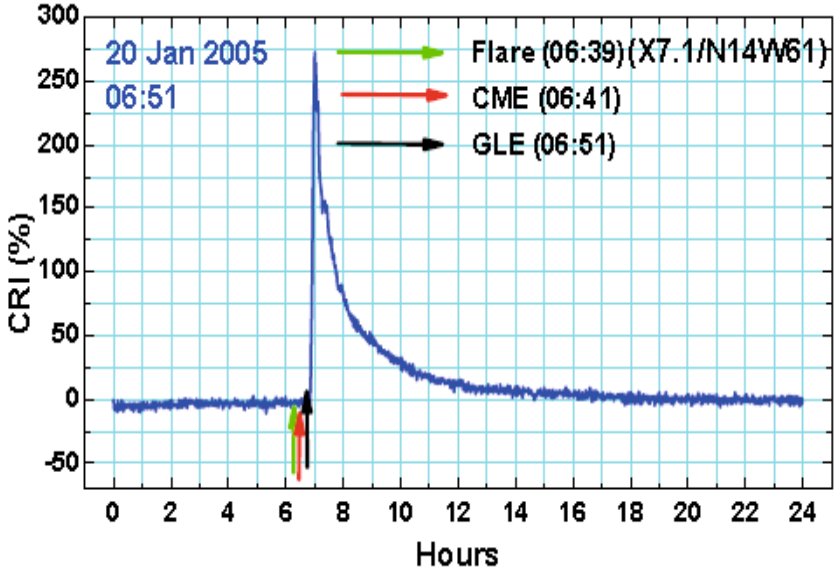

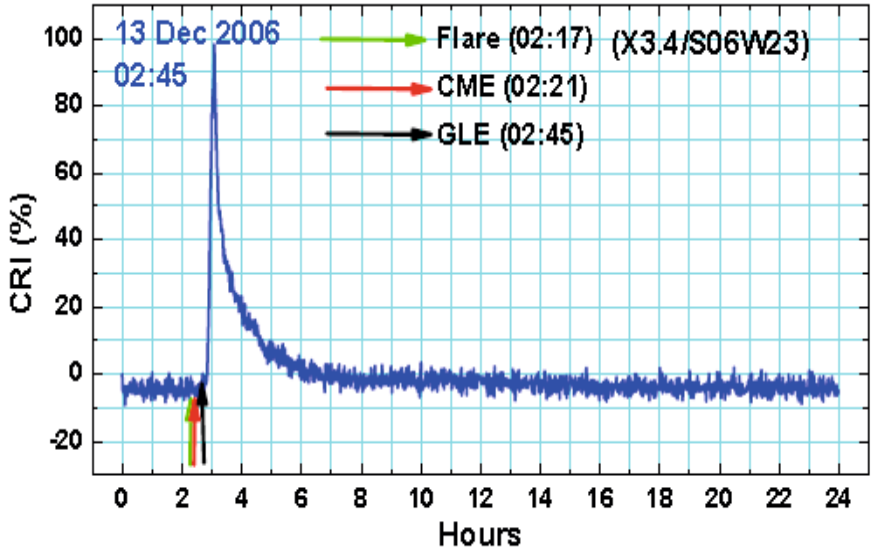

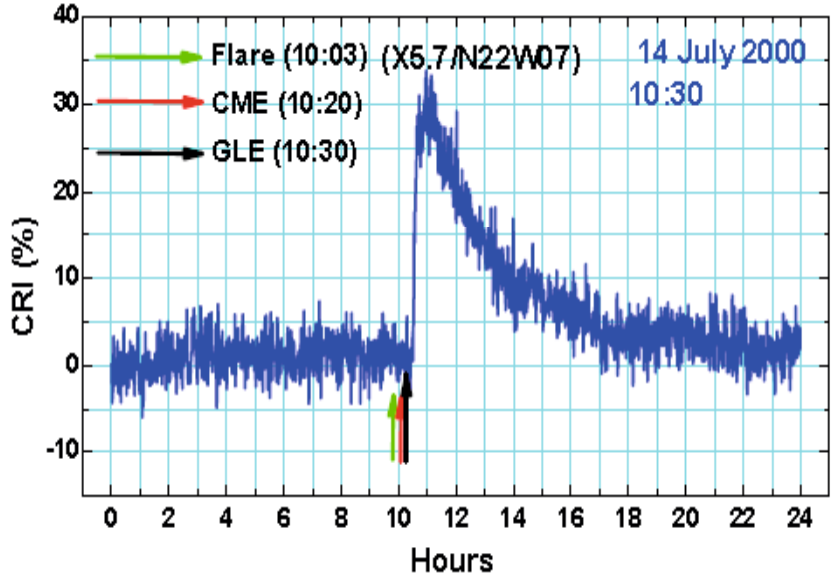

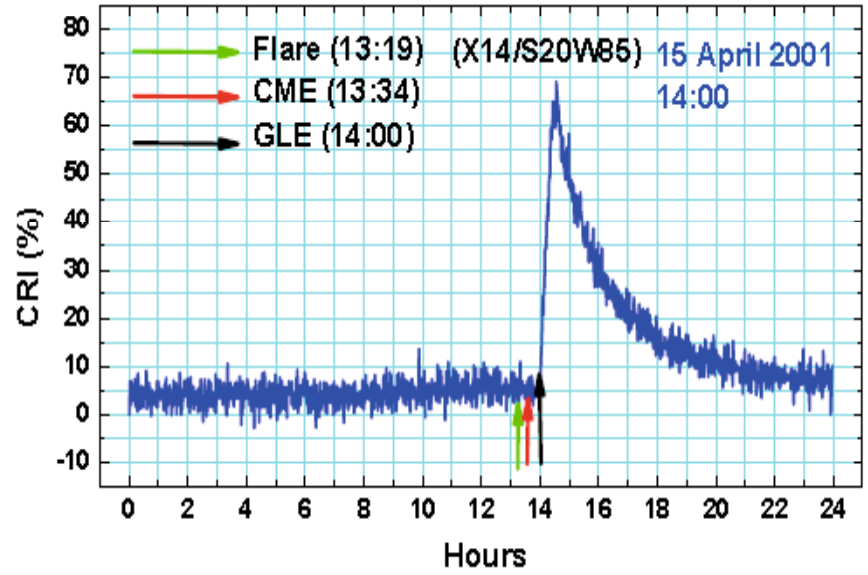

The amplitude of GLE of different events, as observed at various locations (longitudes) on the earth.

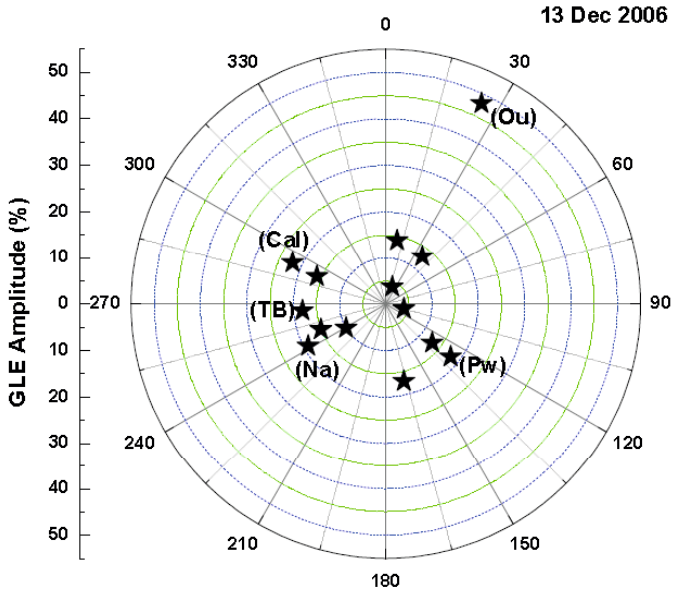

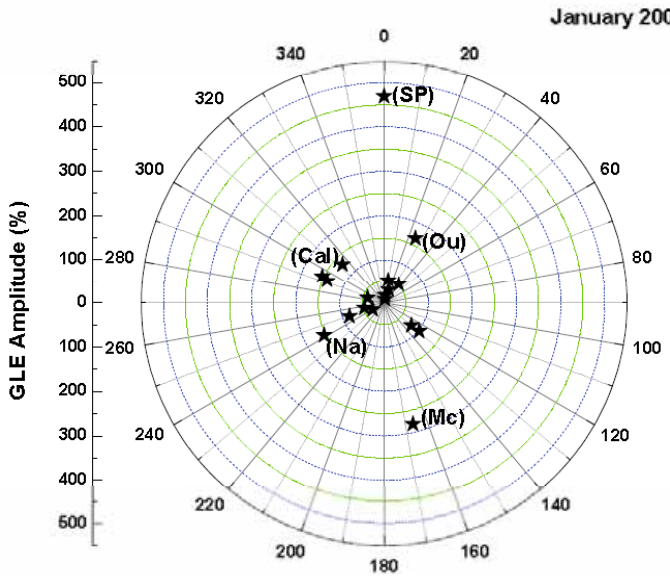

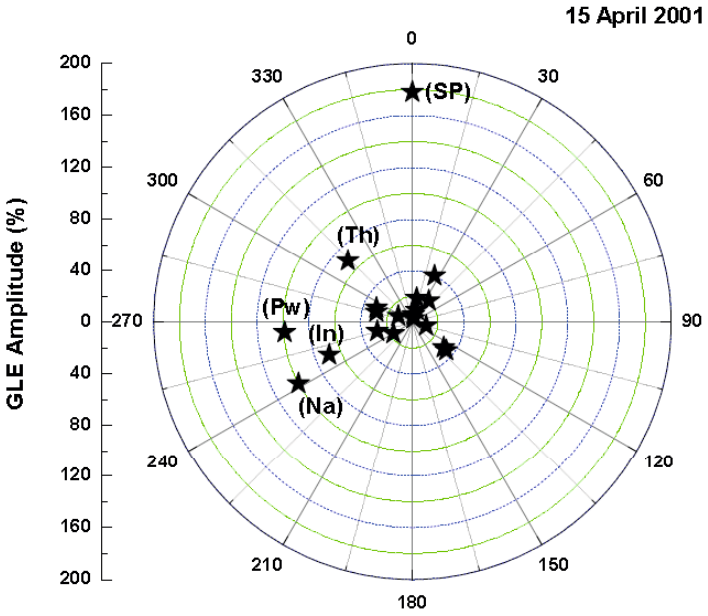

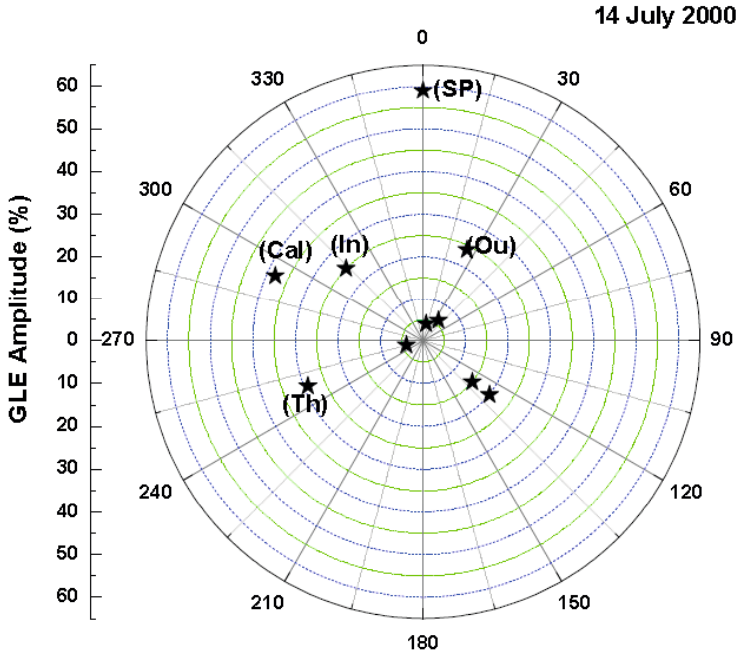

Table: GLEs, variations in their amplitudes at neutron monitors located at different latitudes and longitudes on the Earth; cut off rigidities and median energies of stations is also given.

S.No	NM Station	Lat.	Long.	Alt.(m)	P_c (GV)	E_M (GeV)	GLE (%)							
							13.12. 2006	20.01. 2005	15.04. 2001	14.07. 2000	29.09. 1989	19.10. 1989	22.10. 1989	24.10. 1989
1.	Thule	76.50N	68.70W	260	0.0	10.12	15	84	69	29	343	40	18	86
2.	McMurdo	77.95S	166.6 E	48	0.01	10.12	17	281	---	---	262	41	56	107
3.	South Pole	90.0S	0.0	2820	0.11	10.14	---	469	178	59	346	88	50	189
4.	Inuvik	68.35N	133.7W	21	0.18	10.15	15	130	69	25	338	36	14	92
5.	Fort Smith	60.02N	111.9W	180	0.30	10.17	16	139	30	---	---	---	---	---
6.	Nain	56.55N	61.68W	46	0.30	10.17	19	154	100	---	---	---	---	---
7.	Peawanuck	54.98N	85.44W	53	0.30	10.17	18	---	99	---	----	---	---	---
8.	Tixie bay	71.36N	128.9E	15	0.53	10.23	18	102	31	20	220	28	11	77
9.	Oulu	65.02N	25.5E	15	0.81	10.30	48	165	40	24	164	37	18	93
10.	Calgary	51.08N	114.1W	1128	1.08	10.39	22	153	12	38	345	46	33	103
11.	Yakutsk	62.02N	129.7E	105	1.70	10.64	13	80	34	15	256	26	11	71
12	Newark	39.7N	75.7W	50	1.97	10.76	---	46	28	04	153	---	---	---
13	Kiel	54.3N	10.1E	54	2.29	10.93	14	54	19	04	150	18	15	44
14	Moscow	55.47N	37.32E	200	2.46	11.03	13	54	21	06	179	19	05	52
15	LARC	62.20S	58.96W	40	3.00	11.37	10	30	17	---	---	---	---	---
16.	Climax	39.37N	106.2W	3400	3.03	11.39	---	39	29	---	177	21	09	42
17	Irkutsk	52.28N	104.0E	2000	3.66	11.86	04	---	11	---	---	---	---	---
18	Lomnicky	49.11N	20.13E	2634	4.00	12.14	04	17	10	---	131	09	---	21
19	Jungfraujoch	46.55N	7.98E	3570	4.48	12.57	---	32	06	---	125	05	---	11
20	Hermanus	34.42S	19.22E	26	4.90	12.98	----	08	03	---	93	03	---	08
21	Rome	41.90N	12.50E	60	6.32	14.60	----	---	---	---	78	---	---	----
22.	Almaata	43.14N	76.6E	3340	6.69	15.06	---	---	---	---	101	---	---	---
23.	Tbilsi	41.72N	44.80E	510	6.91	15.37	---	---	---	---	83	---	---	---
24.	Potchefst.	26.68S	27.92E	1351	7.30	15.92	---	---	---	---	80	---	---	---
25.	Beijing	40.04N	116.2E	48	9.56	19.61	---	---	---	---	32	---	---	---
26.	Haleakala	12.03S	75.33W	3400	12.92	26.75								

Variation of amplitude of GLEs, 1) December 13, 2006, 2) Jan 20, 2005, 3) April 15, 2001 and 4) July 14, 2000, with median energy of observing neutron monitors.

- After initial (fast) decrease in GLE amplitude, it decreases rather slowly with increase in median energy of response of neutron monitors

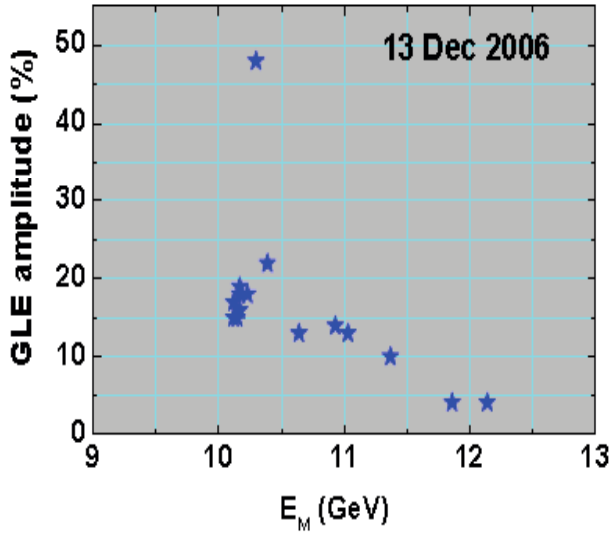

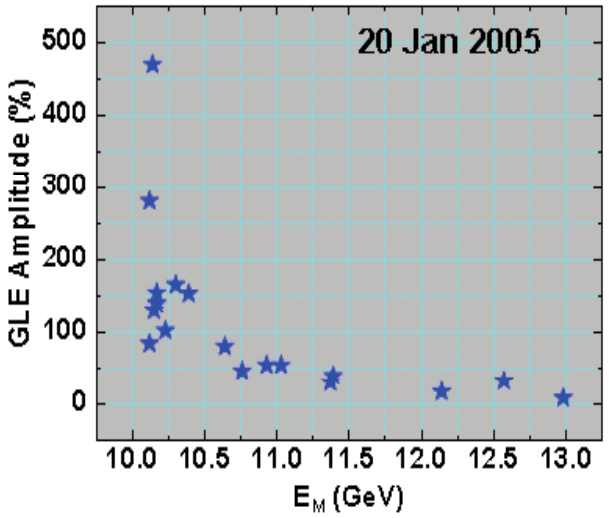

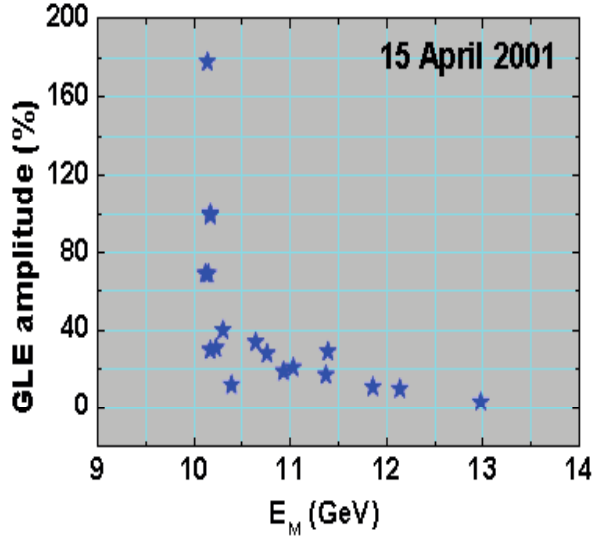

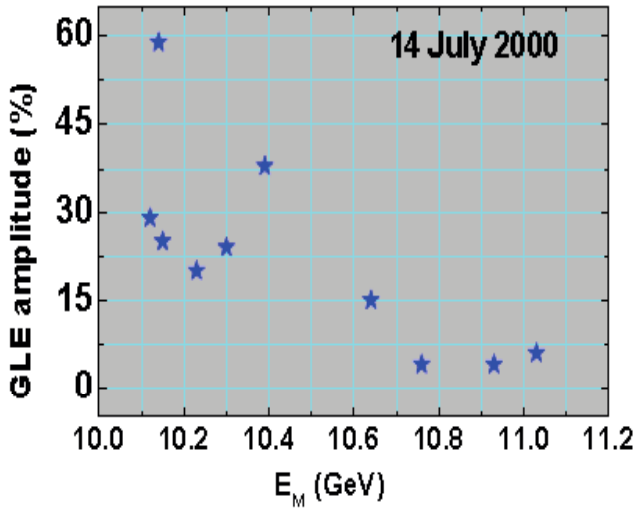

GLE amplitudes (Oulu NM) and ambient GCR conditions during their occurrence

S. No.	GLE date	% (5min- data)	Occurrence during CR level Decreasing/Increasing/Low/Main Phase/Recovery Phase/Normal
1.	28.01.1967	17	Normal
2.	24.01.1971	16	Increasing
3.	01.09.1971	14	Recovery Phase
4.	04.08.1972	10	Main Phase
5.	22.11.1977	13	Normal
6.	07.05.1978	84	Increasing
7.	12.10.1981	11	Recovery Phase
8.	07.12.1982	26	Low
9.	16.02.1984	15	Normal
10.	16.08.1989	12	Recovery Phase
11.	29.09.1989	174	Normal
12.	19.10.1989	37	Low
13.	22.10.1989	17	Recovery Phase
14.	24.10.1989	94	Recovery Phase
15.	21.05.1990	13	Low
16.	24.05.1990	08	Low
17.	26.05.1990	06	Low
18.	28.05.1990	05	Low
19.	15.06.1991	24	Increasing

GLEs (1997-2012), ambient GCR intensity and solar wind plasma/field conditions during their occurrence

S. No	GLE date	% (5min-data)	Occurrence during CR level Decreasing/Increasing/Low /Main Phase/Recovery Phase/Normal	IMF		SD		SW Velocity		Plasma Betta	
				B (nT)	Comment Dec/Inc/low	σ_B (nT)	Comment Dec/Inc/low	V (km/s)	Comment Dec/Inc/low	β	Comment Dec/Inc/low
1.	06.11.1997	11	Low	3.6	low	0.5	low	346	low	1.59	low
2.	02.05.1998	07	Low	11.5	Dec	0.2	low	575	Dec	0.12	low
3.	14.07.2000	30	Recovery Phase	15.5	Inc	5.0	Inc	782	Inc	3.83	Inc
4.	15.04.2001	57	Recovery Phase	2.3	low	0.1	low	503	Dec	4.30	Inc
5.	18.04.2001	05	Recovery Phase	23.8	Inc	5.5	Inc	519	Inc	5.54	Inc
6.	26.12.2001	05	Normal	6.0	low	0.2	low	370	low	2.36	Inc
7.	20.01.2005	269	Recovery Phase	3.4	low	0.2	low	-	-	-	-
8.	13.12.2006	92	Increasing	4.4	Dec	0.1	low	631	Dec	0.41	low
9.	17.05.2012	16	Low	12.1	Inc	0.1	low	352	Dec	0.22	low

- Total GLEs-28

Ambient GCR level when GLE occurred:

- Low intensity =9; Recovery phase of FDs= 9
- Increasing = 4 ; Main Phase = 1; Normal = 5
- 22/28 (≈ 80%) during recovery/increasing or low level of GCR intensity

- In most cases (7/9) IMF is magnetically quiet when GLE occurred

Conclusions

- An ICME or CIR may not be necessary geo-effective as well as GCR-effective, probably due to different mechanisms for generation of GS and FDs.
- CME that develops as sheath/Magnetic cloud structure in interplanetary space appears to be more 'Geo-effective' as well as 'GCR-effective'; However, one-to-one correspondence is not obvious.
- In accord with earlier findings, the most effective interplanetary parameter for geoeffectiveness of ICME appears southward magnetic field/duskward electric field while for CIR geo-effectiveness the north-south fluctuating magnetic field appears important for it to be geoeffective.
- The important interplanetary parameter for 'GCR-effectiveness' appears to be the enhanced and turbulent magnetic field. Scattering of cosmic ray particles by enhanced turbulent magnetic field in the sheath region between the shock and the MC/CME appears to be the most effective mechanism to produce FDs in cosmic radiation. Magnetic field topologies within MC/ICME may further restrict the particle access. Following the passage of shock/sheath/CME structure, the GCR recovers slowly.
- Special attention should be given to analyse CMEs/ICMEs, for their detailed study, which are both 'Geo-effective' and 'GCR-effective'.
- Study of FDs and their precursor anisotropies should be pursued as predictors of arrival shock/ICME and subsequent GS
- *The energy exponent of FDs does not appear to dependent on the level of enhancements in interplanetary parameters and/or responsible interplanetary structures.*
- The amplitude of observed GLE is, in general, higher at lower, and it is lower at higher median rigidity stations. However, the exact nature of dependence is not clear; further study is required in this direction.
- Most of the GLEs occur during recovery phase of FDs and low or increasing GCR intensity
- Most GLEs are observed when interplanetary field condition is quiet at 1 AU.